ForamEcoGEnIE 2.0: Incorporating symbiosis and spine traits into a trait-based global planktic foraminifera model

Rui Ying[1], Fanny M. Monteiro[2], Jamie D. Wilson[1], Daniela N. Schmidt[1]

[1]School of Earth Sciences, University of Bristol, Bristol, BS8 1RJ, UK

5 [2]School of Geographical Sciences, University of Bristol, Bristol, BS8 1SS, UK

Correspondence to: Rui Ying (rui.ying@bristol.ac.uk)

Abstract. Planktic foraminifera are major marine calcifiers in the modern ocean, regulating the marine inorganic carbon pump, and generating marine fossil archives of past climate change. The foraminifera contain ecogroups with and without spines and symbiosis, creating functional trait diversity which expands their ecological niches. Here we incorporate

10 symbiosis and spine traits into the ForamEcoGEnIE model, focusing on functional traits rather than individual species. We calibrated the modelled new traits using Latin Hypercube Sampling and identified the optimal model parameters from an ensemble of 1200 runs compared with global observations from core-top sediment samples, sediment traps, and plankton nets. The model successfully describes the global distribution and seasonal abundance variation of the four major foraminifera functional groups. The model reproduces the dominance of the symbiont-obligate group in subtropical gyres

15 and of the symbiont-barren types in the productive subpolar oceans. Global annual mean biomass and foraminifer-derived carbon export rate are correctly predicted compared to data, with biomass ranging from 0.001 to 0.010 mmol C m^{-3} and organic carbon export 0.002-0.031 mmol C m^{-2} d^{-1}. The model captures the seasonal peak time of biomass and organic carbon export but struggles to reproduce the amplitude of both in productive areas. The sparseness and uneven distribution of observations and the model's limitation in upwelling regions likely contribute to this discrepancy. Our model overcomes

20 the lack of major groups in the previous ForamEcoGEnIE 1.0 version and offers the potential to explore foraminifera ecology dynamics and its impact on biogeochemistry in modern, future and paleogeographic environments.

1 Introduction

Planktic foraminifera are marine calcifying zooplankton that have populated the surface ocean since the mid-Jurassic (~175 Ma). They produce calcite shells (or "tests") preserved in vast amounts in sediments. These sediments provide proxy archives (e.g., ^{13}C, ^{18}O, Mg/Ca) which are commonly used to reconstruct past climate conditions (Tierney et al., 2020), ocean carbonate chemistry (Hönisch et al., 2012), and to study the biotic response to environmental change (Todd et al., 2020). In the modern oceans, foraminifera contribute to 23-56% of the total open-ocean $CaCO_3$ export (Schiebel, 2002) alongside the other major calcifiers, such as coccolithophores (Daniels et al., 2018) and pteropods (Buitenhuis et al., 2019). However, understanding the impacts of environmental change on foraminifera and their role in the carbon cycle is challenged by their low standing stocks in the surface ocean, a (semi)lunar reproductive cycle driving abundances and difficulties in culturing to ground truth physiology (Schiebel and Hemleben, 2017). Modelling planktic foraminifera and their ecology, therefore, has a critical role in increasing and testing our understanding of their biological and ecological influence on the marine inorganic carbon cycle and their role as a paleo-proxy carrier.

Significant developments of global foraminifera models has been driven by the increasing number and extent of flux and community structure observations (Siccha and Kucera, 2017; Buitenhuis et al., 2013; Sunagawa et al., 2020). Most existing models are either empirically-based or focus on selected extant species. For example, Waterson et al. (2017) built a Maxent species distribution model based on sediment core data to study the niche variability during the Last Glacial Maximum (LGM) compared to the Holocene. Žarić et al. (2006) constructed a statistical model that correlated hydrographical factors with sediment trap abundance of 18 dominant species. Correlative models, though, are limited for extensive future projections as they assume a constant environmental niche, neglecting adaptation and acclimation (Buckley et al., 2010). In addition, niche models do not resolve biological interactions which have an important role in shaping species distribution (Anderson, 2017).

Fraile et al. (2008, 2009), Lombard et al. (2011) and Kretschmer et al. (2016, 2018) built and extended ecophysiology-based models (PLAFOM and FORAMCLIM) to overcome these limitations. They successfully reconstructed planktic foraminifer's geographical distribution, seasonal and vertical population dynamics and simulated distributions in different climatologies such as the LGM (Fraile et al., 2009) and future high-emission scenarios (Roy et al., 2015). Both models are species-based and therefore cannot be applied in the deeper geological record older than the Miocene (>5 Ma) (Kucera and Schonfeld, 2007), due to a high number of extinct species and cryptic taxa with unknown novel ecologies (Renaud and Schmidt, 2003). Additionally, FORAMCLIM uses experimental growth rates to simulate foraminifera abundance and does not resolve top-down controls on foraminifera biomass. To fill the model gap and to leverage the abundant foraminifer fossil information, a mechanistic model not limited to species is needed.

Trait-based plankton models are an alternative approach focusing on organismal traits including morphological and physiological properties instead of taxonomic identities. They provide a mechanistic way to mimic the complex ocean ecology characterising the functional groups, their traits and associated benefits and costs (i.e., trade-offs) (Zakharova et al., 2019; Kiørboe et al., 2018). Models adopting trait-based approaches have successfully reconstructed the biomass distribution of diverse marine community including cyanobacteria (Follows et al., 2007) and diazotrophs (Monteiro et al., 2010). This modelling strategy is well suited to be applied to planktic foraminifera as functional traits such as body size (Schmidt et al., 2004a), size normalised weight (Todd et al., 2020; Barker and Elderfield, 2002), and symbiosis (Spero and Parker, 1985) are widely measured and studied. The evolution of these functional traits has been described in detail across the Cenozoic (Ezard et al., 2011).

Critical traits of planktic foraminifera include calcification, body size, presence and absence of spines and symbiosis. While calcification and body size are universal traits for all foraminifera, the evolution of spines and symbiosis determine the species-level discrepancies (Aze et al., 2011). Based on the presence of symbionts and spines, foraminifera can be divided into four functional groups: (1) symbiont-barren non-spinose; (2) symbiont-barren spinose; (3) symbiont-facultative non-spinose; (4) and symbiont-obligate spinose (Table 1). Roughly 19 out of the 50 modern foraminifer species are symbiotic, bearing eukaryotic algae such as dinoflagellates, chrysophytes and haptophytes (Takagi et al., 2019), though this important relationship is not established for all taxa. Photosynthesising symbionts provide extra energy to foraminifera in nutrient-depleted regions (LeKieffre et al., 2018; Ortiz et al., 1995; Uhle et al., 1999). Consequently, symbiotic species dominate tropical to subtropical regions, while non-symbiont species (termed as "symbiont-barren") reach high abundance in temperate and polar oceans (Figure 3). Some symbiont bearing taxa cannot live without their symbionts (termed as "symbiont-obligate") (Bé et al., 1982) while others are flexible (termed as "symbiont-facultative").

The presence of calcareous spine influences the foraminifera's feeding behaviour. Non-spinose foraminifera rely on rhizopodia to capture prey. Spinose foraminifer have spines extruding from the test increasing their effective reach range and ability to active prey, which increases the ability to caption more prey types and larger cell sizes like copepods (Anderson et al., 1979). Laboratory observations show that spinose carnivory foraminifera prefer food with a high zooplankton-to-phytoplankton protein ratio (Schiebel and Hemleben, 2017). The effective encounter rate of a spinose taxon can be three orders of magnitude higher than non-spinose species (Gaskell et al., 2019). Roughly half of modern species are spinose but existing models have not taken this trait advantage into consideration.

Recently, Grigoratou et al., (2019) developed the first mechanistic and trait-based 0D model (ForamEcoGEnIE 1) for the symbiont-barren non-spinose foraminifer group and coupled it to cGEnIE (Grigoratou et al., 2021a), a 3D Earth System Model of Intermediate Complexity (EMIC) allowing for fast computational time and widely applied to past climates including the Palaeocene–Eocene Thermal Maximum (Ridgwell and Schmidt, 2010), Last Glacial Maximum (Rae et al.,

2020) and Cretaceous-Paleogene boundary (Henehan et al., 2019). The computational efficiency and application to a wide range of geological periods mean ForamEcoGEnIE can be used to explore foraminifer diversity in past climates beyond the limits of other models (Ezard et al., 2011). Here, we extend the previous model to ForamEcoGEnIE 2.0 by resolving 3 more critical functional groups of planktic foraminifera by adding the traits of symbiosis and spines (the latter tested in Grigoratou et al., 2021b). We tuned the model by comparing with three global observational data compilations (sediment core-tops, plankton nets and sediment traps) and test its ability to reproduce surface biomass, organic carbon and calcite flux, and geographic distribution in the modern climate.

2 cGEnIE ocean and atmosphere physics

ForamEcoGEnIE is based on cGEnIE (carbon-centric Grid-ENabled Integrated Earth system model). The fast climate and ocean physics of cGEnIE are based on a coarse-resolution 3D frictional geostrophic ocean model coupled to a 2D energy-moisture-balance atmosphere model and a dynamic-thermodynamic sea-ice model (Edwards and Marsh, 2005; Marsh et al., 2011). The ocean has a 36x36 equal-area horizontal grid (uniform in longitude and sine-uniform in latitude) with 16 logarithmically spaced vertical levels as defined in Cao et al., (2009). The physical model is coupled with a model of ocean biogeochemical cycles (Ridgwell et al., 2007; van de Velde et al., 2021), sea-floor sedimentary processes (Ridgwell and Hargreaves, 2007) and marine ecosystem processes (Ward et al., 2018). The plankton ecosystem is resolved in the surface layer (0-80.8 m). The model presented in this study is configured with a seasonally forced pre-industrial climate state and an atmospheric CO_2 concentration restored to 278 ppm.

3 Size-based plankton ecosystem framework EcoGEnIE

3.1 Biogeochemical tracers

The model has three main state variables: inorganic resources (i_r), living biomass (i_b), and detritus (i_d). Each state variable contains multiple biogeochemical tracers: carbon, phosphorus, iron. Plankton populations are counted in notation j, and each plankton includes the three tracers above, although autotroph planktons (phytoplankton and symbiotic foraminifera) have an extra tracer of chlorophyll (noted in Chl). Figure 1 shows a schematic of the plankton types including foraminifera and denotes elements in different colours.

3.2 Plankton cell size and quota

In EcoGEnIE, individual body size determines key physiological processes including nutrient uptake, photosynthesis, grazing gain, and predation through allometric scaling (West et al., 1997), because of its role as a master trait among pelagic organisms (Andersen et al., 2016). The modelled size-dependent parameters (except for photosynthesis) follow a generic power law: $P = aV^b$ with P the size-based parameter, V the spheric biovolume, and a, and b the allometric intercept and exponent.

A fundamental size-based concept of EcoGEnIE is the plankton cell quota for various elements. The carbon quota content (Q_C) follows the same power law as per Equation 1. Variable stoichiometry (Q_{i_b}, Eqn. 2) is achieved by the ratio of assimilated nutrients biomass (B_{i_b}, where i_b stands for P, Fe, or chlorophyll) to carbon biomass (B_C) (Droop, 1968; Flynn, 2008). This stoichiometry limits nutrient uptake rate ($Q_{i_b}^{stat}$, Eqn. 3) as per Geider et al., (1998), with higher value close to its maximum ($Q_{i_b}^{max}$) lowering the nutrient uptake or chlorophyll synthesis rate. The nutrient quota range ($Q_{i_b}^{min}$, $Q_{i_b}^{max}$) is proportional to the carbon quota (Q_C).

$$Q_C = aV^b \tag{1}$$

$$Q_{i_b} = \frac{B_{i_b}}{B_C}, \qquad i_b = P, Fe, Chl \tag{2}$$

$$Q_{i_b}^{stat} = \left(\frac{Q_{i_b}^{max} - Q_{i_b}}{Q_{i_b}^{max} - Q_{i_b}^{min}} \right)^{0.1} \tag{3}$$

3.3 Plankton biomass dynamics

The biomass of any plankton group (j) and element (i_b), B_{j,i_b}, varies due to a combination of potential physiological processes that are determined by the type of organism: nutrient uptake, grazing gains, grazing losses, mortality, and respiration loss (Eqn. 5). Foraminifer-related specific processes will be introduced in following sections. We refer readers to Ward et al. (2018) for the detailed description of EcoGEnIE that expands on the description below.

$$\frac{\partial B_{j,i_b}}{\partial t} = \underbrace{\mu_{j,i_b} \cdot B_{j,C}}_{nutrient\ uptake} + \underbrace{B_{j,C} \cdot \lambda_{i_b} \sum_{j_{prey}=1}^{J} G_{j,j_{prey},i_b}}_{grazing\ gains}$$

$$\underbrace{- B_{j_{pred},C} \cdot \sum_{j_{pred}=1}^{J} G_{j_{pred},j,i_b}}_{grazing\ losses} - \underbrace{m_j \cdot B_{j,i_b}}_{mortality\ loss} - \underbrace{r_{j,C} \cdot B_{j,i_b}}_{respiration\ loss} \tag{4}$$

3.4 Inorganic nutrient dynamics

The inorganic resource state variables (R_{i_r}) varies with nutrient uptake (V_{j,i_r}) and dissolved inorganic carbon (DIC) with the living organisms' respiration ($r_{j,C}$).

$$\frac{\partial R_{i_r}}{\partial t} = \begin{cases} \sum_{j=1}^{J} -\mu_{j,i_r} \cdot B_{j,C}, & i_r = Fe, P \\ \sum_{j=1}^{J} -\mu_{j,i_r} \cdot B_{j,C} + \sum_{j=1}^{J} r_{j,C}, & i_r = C \end{cases} \tag{5}$$

Additional sources and sinks of nutrients such as remineralisation of organic matter and air-sea gas exchange are computed in the biogeochemical module BIOGEM (Ridgwell et al., 2007).

3.4 Particulate Organic matter dynamics

Particulate Organic matter flux (F) is a combination of predators' messy feeding (the first term) and the mortality loss (the second term) from all plankton groups (Eqn. 6).

$$F = \sum_{j_{pred}=1}^{J} \sum_{j_{prey}=1}^{J} (1 - \beta_{j_{pred,i_d}})(1 - \lambda_{j_{pred,i_b}})\, G_{j_{pred},j_{prey}}\, B_{j_{pred,\,C}}$$
$$+ \sum_{j=1}^{J} (1 - \beta_j)\, m_j\, B_{j,i_d} \tag{6}$$

$\beta_{j_{pred}}$ is the fraction of dissolved organic matter (DOM) subject to diffusion and advection by ocean circulation. The remaining fraction $(1 - \beta_{j_{pred}})$ is the particulate organic matter (POM) subject to redistribution through the water column by sinking. The parameter β is a sigmoid function depending on maximum and minimum DOM fraction (β_{max}, β_{min}) of predators' ESD and the size β_s at which DOM/POM ratio equals 1 (Ward and Follows, 2016). Smaller cell sizes are associated with greater proportion as DOM.

$$\beta = \beta_{max} - \frac{\beta_{max} - \beta_{min}}{1 + \beta_s/ESD} \tag{7}$$

Messy feeding behaviour is modelled as the unassimilated fraction $(1 - \lambda_{j_{pred}})$ of prey which is limited by the size-independent maximum efficiency coefficient (λ_m) and the nutrient limitation (Fe or P).

$$\lambda = \lambda_m \cdot min[Q_P^{stat}, Q_{Fe}^{stat}] \tag{8}$$

4 ForamEcoGEnIE 1 brief description

ForamEcoGEnIE 1 accounted for the feeding behaviour and calcification of foraminifera (Grigoratou et al., 2019, 2021a). It implemented a predator-prey interaction ($G_{j_{pred},j_{prey}}$, Eqn. 9) using a Holling type II model (Holling, 1965), where the overall grazing rate depends on the total available prey ($F_{j_{pred}}$), the maximum grazing rate of predators (G_{pred}^m) and the half-saturation concentration of available food ($k_{j_{prey}}$), and is regulated by temperature limitation (γ_T), a prey-switching term (Φ), and a prey refuge protection ($1 - e^{\Lambda F_{j_{pred}}}$). The calcification trait was included by reducing foraminifera palatability (P_p which influences $F_{j_{pred}}$, Eqn. 10) and mortality rate (m_j, Eqn. 5) to account for higher protection against predators and infections to the expense of a lower G_{foram}^m (Eqn. 9). We also introduce the ForamEcoGEnIE 2 parameters (spine effect τ and a mixotrophy limitation λ_h) here, which is set to 1, i.e., not functioning in ForamEcoGEnIE 1.

$$G_{j_{pred},j_{prey}} = \underbrace{\gamma_T \cdot \lambda_h}_{\text{limitations}} \cdot \underbrace{\frac{G_{pred}^m F_{j_{pred}}}{\tau k_{j_{prey}} + F_{j_{pred}}}}_{\text{overall grazing rate}} \cdot \underbrace{\Phi_{j_{pred},j_{prey}}}_{\text{Switching}} \cdot \underbrace{\left(1 - e^{\Lambda F_{j_{pred}}}\right)}_{\text{prey refuge}} \tag{9}$$

$$F_{j_{\text{pred}}} = P_p \cdot B_{j_{\text{prey}}} \cdot exp\left[-\left(ln\left(\frac{\mu_{j_{\text{pred}},j_{\text{prey}}}}{\mu_{\text{opt}}}\right)\right)^2 / (2\sigma_{j_{\text{pred}}}^2)\right] \tag{10}$$

Predators select their prey (Eqn. 10) based on the predator-prey size ratio $\mu_{j_{\text{pred}},j_{\text{prey}}}$ relative to the optimal value μ_{opt}, the predators' food range $\sigma_{j_{\text{pred}}}^2$, and the calcification protection P_p. Foraminifera in both ForamEcoGEnIE 1 and 2 are set as herbivores.

The grazing process like other metabolic processes in EcoGEnIE are temperature dependent, following the universal metabolic theory (Brown et al., 2004). The body temperature of ectothermic plankton is determined by the ambient seawater environment (T). Temperature regulation γ_T acts on metabolic processes including respiration, nutrient uptake, and predation. It is modelled through an Arrhenius-like function (Eqn. 12), where the parameter A determines temperature sensitivity and reference temperature (T_{ref}) is the temperature allowing $\gamma_T = 1$.

$$\gamma_T = e^{A(T-T_{\text{ref}})} \tag{11}$$

The prey-switching term ($\Phi_{j_{\text{pred}},j_{\text{prey}}}$) simulates the feeding habitat of zooplankton (Eqn. 9). The exponential s defines the active level of zooplankton predators, which capture abundant prey with higher priority when s increases. Foraminifera both in ForamEcoGEnIE 1 and 2 are assumed to be ambush passive predators with s=1.

$$\Phi_{j_{\text{pred}},j_{\text{prey}}} = \frac{\left(F_{j_{\text{pred}}}\right)^s}{\sum_{j_{\text{prey}}=1}^{J}\left(F_{j_{\text{pred}}}\right)^s} \tag{12}$$

A refuge term $(1 - e^{\Lambda F_{j_{\text{pred}}}})$ in Eqn. (9) is added to decrease the grazing rate when prey availability lowers. The coefficient Λ determines the strength of such protection.

5 ForamEcoGEnIE 2: improved calcification and more functional groups

In ForamEcoGEnIE 2, we add symbiosis and spine traits for foraminifera to result in four functional groups (Table 1, Figure 1). We also implement a new calcification energetic cost by using a respiration term rather than a reduced maximum growth rate in ForamEcoGEnIE 1.

Table 1. The four modelled functional groups of planktic foraminifera and their species representative in ForamEcoGEnIE 2.0.

Spine trait	Symbiosis trait	Species example	Species number*	Model implementation
Spinose	Symbiont-obligate	*Globigerinoides ruber*	17	This study
Spinose	Symbiont-barren	*Globigerina bulloides*	2	This study

| Non-spinose | Symbiont-facultative | *Neogloboquadrina dutertrei* | *5* | This study |
| Non-spinose | Symbiont-barren | *Neogloboquadrina pachyderma* | 23 | extended from ForamEcoGEnIE 1 |

* Count from Schiebel and Hemleben (2017)
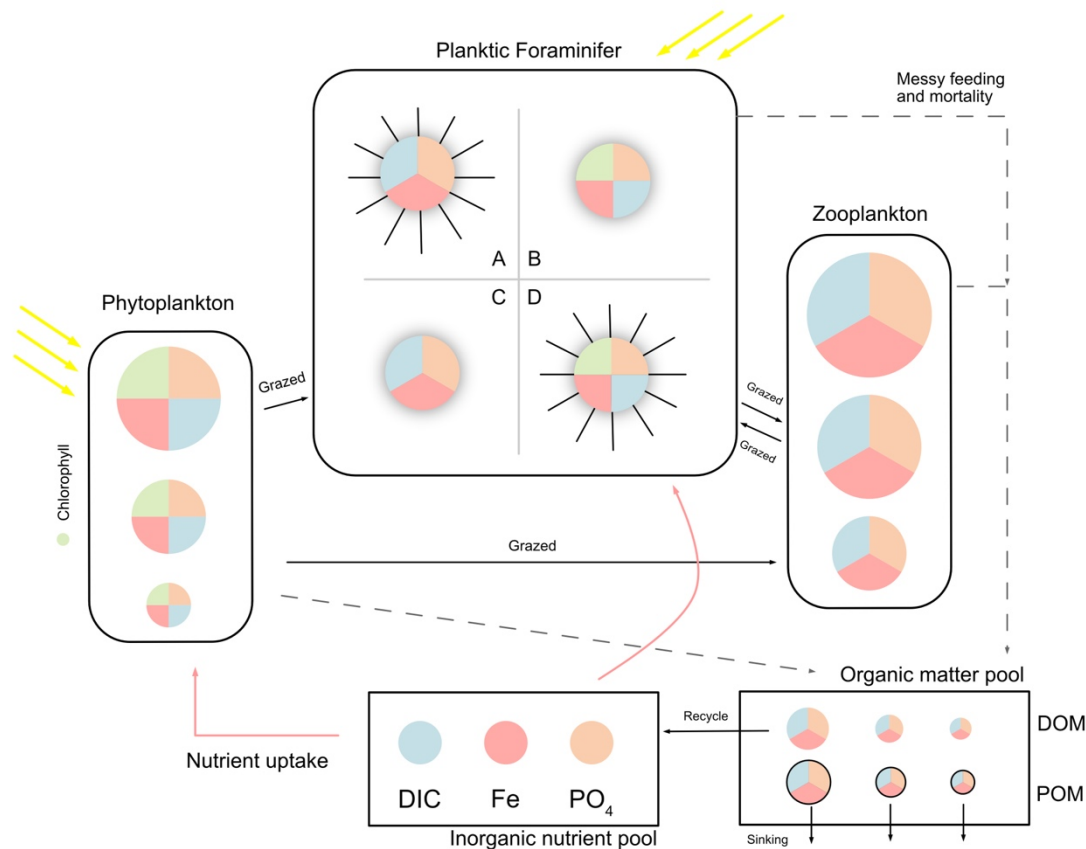
195

Figure 1. Schematic of ForamEcoGEnIE 2.0 model structure. The model includes the biogeochemical cycles of C, Fe and P (shown in different colours), various plankton size classes and four main groups of planktic foraminifera: A. symbiont-barren spinose group; B. Symbiont-facultative non-spinose group; C. symbiont-barren non-spinose group. D. symbiont-obligate spinose group. DIC stands for dissolved inorganic carbon and PO₄ for phosphate. The model
200 **represents nutrient uptake (red arrows), dissolved and particulate organic matter production (DOM and POM) caused by messy feeding and mortality (dashed arrows), and zooplankton grazing (black arrows).**

5.1 Calcification trait trade-offs

5.1.1 Benefit: Mortality protection

205   The mortality loss term for zooplankton scales with a basal rate constant m_b (Eqn. 5). As per Grigoratou et al. (2019, 2021a), m_b this is downscaled for foraminifera by a protection term P_m where a lower value of m_j indicates a higher protection from the foraminifera test against viral and bacterial infections.

$$m_j = P_m \cdot m_b \tag{13}$$

210   5.1.2 Benefit: Protection from predators (palatability)

As per ForamEcoGEnIE 1.0, calcification protects from grazing and is defined by P_p, which reduces the biomass loss from predation (Eqn. 10).

5.1.3 Cost: higher metabolic cost

215   We modified the metabolic cost of calcification defined in Grigoratou et al. (2019, 2021a) by replacing the original reduced maximum growth rate (or specifically maximum grazing rate) with a temperature-dependent respiration loss term. We made this change because (1) extra respiration is a more biologically realistic cost with (2) this temperature-dependent term reconciling the model with the low-latitude biomass observation. The respiration r_j present in Eqn. 5 scales with carbon biomass and is multiplied by constant r_b and temperature limitation (Eqn. 11). We assumed that the lost carbon from

220   respiration is instantly recycled back to dissolved inorganic carbon (DIC) pool.

$$r_j = r_b \cdot \gamma_T \tag{14}$$

5.2 Spine trait trade-offs

Spines are an important part of foraminiferal taxonomy. Spines like the overall test are made of calcite. A range of biological

225   functions are assumed linked to symbiosis and feeding behaviour (Schiebel and Hemleben, 2017).

5.2.1 Benefit: Enhanced grazing

Studies show that spinose foraminifera are more efficient in capturing and digesting prey due to the spine and rhizopodia networks (Anderson and Bé, 1976). Spines widen the prey availability of immotile foraminifer and facilitate capturing larger

230   preys. Non-spinose species cannot hold active prey and only accept smaller particles of copepods in the laboratory observations (Anderson et al., 1979; Hemleben et al., 1989). Grigoratou et al. (2021b) modelled such benefit by reducing the half-saturation constant (conventionally noted as k in a Michaelis-Menten model). Here we adopt this approach by reducing k_{j_prey} by a scaling parameter τ ($0 < \tau < 1$; Eqn. 10).

235   5.2.2 Other trade-offs as calcification: higher metabolic cost and reduced palatability

We assume that the metabolic cost and protection from the spines are characterised the same way as for calcification (Eqn. 13-14). Spinose foraminifera have a higher cost for calcification due to the slightly higher amounts of carbonate and a

stronger protection than non-spinose taxa (Table 2). We did not reduce the mortality term as this not supported by direct evidence.

240

5.3 Symbiosis trait trade-offs

Symbiosis is a novel trait in the model, commonly seen in marine organisms including foraminifer. Many planktic foraminifera harbour algae (e.g., dinoflagellate, diatom) within their cell (Takagi et al., 2019). We represent these symbiotic species in the model as a single organism, which combines hetero- and autotrophy, equivalent to a calcifying mixotroph. We

245 use the trait-based representation of mixotrophy of Ward and Follows (2016), where any plankton can "naturally" predate and photosynthesize. While mixotrophs have this ability in the model, this is turned off for the rest of plankton (i.e., V_m is 0 for zooplankton and G_m is 0 for phytoplankton).

5.3.1 Benefit: enabled autotrophy for planktic foraminifer

250 The symbiont has a cell size that is defined via a symbiont/foraminifera size ratio ψ (Eqn. 16) to characterise the symbiont's affinity in taking up nutrients and light. Photomicrograph observations showed that foraminifera symbionts are about 1:20 smaller in size than the host cell (Takagi et al., 2019).

$$V_s = \psi^3 V_h \tag{15}$$

The generic nutrient uptake of symbionts follows a mixotrophy- (λ_s), quota- ($Q_{i_r}^{\text{stat}}$) and temperature-limited (γ_T) Michaelis-

255 Menten function where the variable (**R**) represents nutrient resources. The half-saturation constant is replaced by nutrient affinity, a more mechanistic parameter for nutrient uptake α_{ir}. Nutrient affinity is often referred to "clearance rate" and regarded as a proxy of competitive strength (Fiksen et al., 2013). According to Edwards et al. (2012) review on phytoplankton trait trade-offs, nutrient affinity is negatively related to cell size because of lower surface to volume ratio, while maximum uptake rate (V_m) is positively related.

260
$$\mu_{i_r} = \lambda_s \cdot Q_{i_r}^{\text{stat}} \cdot \gamma_T \cdot \frac{V_{i_r}^m \alpha_{i_r} \mathbf{R}}{V_{i_r}^m + \alpha_{i_r} \mathbf{R}} \tag{16}$$

The symbionts' photosynthesis growth is modelled following a size-dependent unimodal equation (Geider et al., 1998; Moore et al., 2001). This equation has higher explanatory power for eukaryotes phytoplankton cells than a power law (Bec et al., 2008). The maximum photosynthesis rate P_C^m is determined by dimensionless parameter P_a, P_b, P_c and the biovolume of symbiont V_s, and the mixotrophy cost λ_s.

265
$$P_C^m = \frac{\lambda_s (P_a + log_{10} V_s)}{P_b + P_c log_{10} V_s + log_{10} V_s{}^2} \tag{17}$$

The practical photosynthesis rate is further constrained by nutrient availability (the smallest between γ_{Fe} and γ_P), temperature (γ_T), and light intensity (γ_I).

$$P_C = P_C^m \cdot \min[\gamma_P, \gamma_{Fe}] \cdot \gamma_T \cdot \gamma_I \tag{18}$$

Nutrient limitation γ_{i_r} (i_r is either P or Fe, see the definition in Eqn. 2) is determined by the minimal value of the phosphorus or iron limitation term, which follows the quota relationship in Droop (1968).

$$\gamma_{i_r} = \frac{1 - Q_{i_r}^{\min}/Q_{i_r}}{1 - Q_{i_r}^{\min}/Q_{i_r}^{\max}}, \quad i_r = \text{Fe, P} \tag{19}$$

Light limitation, follows the model of Moore et al. (2001) where I represents light intensity, α is initial slope of P-I curve limited by Fe content (γ_{Fe}), and Q_{Chl} is chlorophyll quota.

$$\gamma_I = 1 - \exp\left(\frac{-\alpha \cdot \gamma_{Fe} \cdot Q_{\text{Chl}} \cdot I}{P_C^m \cdot \gamma_T \cdot \min[\gamma_P, \gamma_{Fe}]}\right) \tag{20}$$

5.3.2 Cost: downgrading autotroph and heterotroph efficiency

The cost of mixotrophy is that both autotrophic and heterotrophic processes (i.e., photosynthesis and grazing rates) are scaled down (by multiplying factor λ_s and λ_h respectively for symbionts and hosts, $0 < \lambda_s, \lambda_h < 1$, Eqn.9 and 16) compared to the pure auto/heterotroph specialist (Castellani et al., 2013; Våge et al., 2013; Ward and Follows, 2016). We distinguish between symbiont-obligate and symbiont-facultative foraminifera using different λ_s/λ_h parameter values to reflect their different dependency on symbionts (Table 2).

5.4 Approximating foraminifera calcite export

Planktic foraminifera produce organic carbon in the subsurface water column (Salter et al., 2014) and sequester inorganic carbon into the deep oceans via their dead tests (Schiebel, 2002). The organic carbon flux derived from foraminifera is treated the same way as in EcoGEnIE as discussed in section 3.4. The calcite export, specific to foraminifera, is approximated by multiplying the foraminifera bulk organic carbon export with a globally uniform particle inorganic carbon (PIC) to organic carbon (POC) ratio of 0.36 based on the empirical data by Schiebel and Movellan (2012).

6 Model parameterisation

6.1 Plankton community size structure

We resolve eight size classes of phytoplankton, seven size classes of zooplankton and one size class for each of the four foraminifer groups. Phytoplankton and zooplankton size classes include 0.6, 1.9, 6.0, 19.0, 60.0, 190.0, 600.0 and 1900.0 μm, with zooplankton missing the smallest class due to minimum prey size. While the size structure of these planktons is fixed, we tested the foraminifer ESD ranging from pre-adult (60 μm) to adult (600 μm) using the ensemble described below. Each test contains one randomly assigned foraminifer size and this is same for each foraminifera group. However, we found the size (190 μm) from previous study (Grigoratou et al. 2021) still achieved the best score (Table 2).

6.2 Experiments with sampled parameters

We run an ensemble of 1,200 model experiments, each testing a different combination of parameter values (Table 2), to explore all possible trait values and select the best trait combinations to match available foraminifera observations (section 3.2). The parameter sets are generated using a Latin Hypercube Sampling (LHS) algorithm that samples values of 12 foraminiferal parameters from uniform parameter distributions (Table 2; Sarrazin et al., 2016). However, several rules are set in the sampling: (1) the spinose ones always own higher palatability and mortality protection (and corresponding respiration cost) than the non-spinose ones; (2) the symbiont size for both symbiont-facultative and symbiont-obligate group are set to the same value; (3) all the foraminifera have the same size. Each simulation is run for 250 years continuing from a 10,000-year spin-up simulation as ecosystem structure typically reaches equilibrium after ~50 years. The other ecosystem parameters are the same as Ward et al. (2018) (Table S3).

Table 2: List of the foraminifer-relevant model parameters tested in the global sensitivity analysis (GSA) and identified optimal parameter values for each foraminifera group.

Related trait(s)	Parameter	Description	Tested range[1]	Unit	Optimal values (bn[2])	Optimal values (bs[2])	Optimal values (sn[2])	Optimal values (ss[2])
Foraminifer Size	ESD	Equivalent Sphere Diameter	[60, 600]	μm	**190**[3]	190	190	190
Calcification/spine	p_m	Protection from mortality	[0-1]		**0.6**	0.6	0.6	0.6
	p_p	Protection from grazing	[0-1]		**0.8**	**0.7**	0.8	0.7
	r	Respiration rate	[0-0.02]	mmol C d^{-1}	**0.04**	**0.06**	0.04	0.06
Spine	τ	coefficient of grazing half saturation	[0-1]		/	**0.9**	/	0.9
Symbiosis	ψ	symbiont to foraminifer size ratio	[0-0.05]		/	/	**0.0015**	0.0015
	λ_s	symbiont autotroph efficiency	[0-1]		/	/	**0.2**	**0.8**
	λ_h	foraminifer heterotroph efficiency	[0-1]		/	/	**0.8**	**0.55**

[1] All scaling parameters are sampled from values of 0 to 1; respiration terms are as per Ward et al. (2018); the symbiont cell size ratio upper bound is calculated from Takagi et al., (2019). For any other plankton group where these traits are not relevant, scaling parameters are set to 1 and cost parameters are set to 0.

[2] bn, symbiont-barren non-spinose; bs, symbiont-barren spinose; sn, symbiont-facultative non-spinose; ss, symbiont-obligate spinose

[3] The bold parameters are also shown in other groups with same trait(s).

6.3 Observations for comparison

6.3.1 Relative abundance

We used a sediment core-top census data compilation (Siccha and Kucera, 2017) to represent a long term mixed Late Holocene baseline (pre-industrial) to validate the spatial abundance patterns of each modelled foraminifer group. We calculated the modelled relative abundance of each group based on its carbon export production.

To determine the observed relative abundance, we compiled species into functional groups using species traits defined by Schiebel and Hemleben (2017) and Takagi et al. (2019) (Table S4). We regridded the observations into the model grid

(averaging each data grid point onto the cGEnIE grid). We ignored species with less than 3% local abundance (a few specimen) to avoid uncertainties caused by transport via ocean currents (van Sebille et al., 2015) and taxonomic uncertainties of rare taxa. This threshold is determined by the standard error of the fisher's diversity index (Fisher et al., 1943). We used the Mielke measure (details in Section 6.3) to quantify the model-data fit. We omitted the Arctic Ocean and the Mediterranean Sea in the model-data comparison because the model resolution in these regions is too low to represent adequate ocean physics.

6.3.2 Annual average biomass and export

To validate the modelled biomass and organic carbon export, we compiled two global datasets: (1) plankton net data from the first 100 m (if sampled, otherwise the nearest depth that is no more than 120 m) for biomass and (2) sediment trap data for carbon export. We converted the units of plankton net ("number m^{-3}") and sediment trap data ("number m^{-2} d^{-1}") into "mmol C m^{-3}" and "mmol C m^{-2} d^{-1}" using the empirical factor of 0.845 µg specimen^{-1} from Schiebel and Movellan (2012). We converted modelled carbon export production (mmol C m^{-3} d^{-1}) into "mmol C m^{-2} d^{-1}" multiplying by the surface-layer depth (80.8 m) to compare with sediment-trap-generated export observations. The full list of plankton net and sediment trap data sources is in Tables S1 and S2.

Both datasets are classified by species and were regridded into the model resolution following the methods of the core-top data. We calculated the annual average at each grid point to remove seasonality and interannual variability. However, the plankton nets are mostly sampled within one month (Figure S1), and represent a day's snapshot, such that the annual mean biomass is likely overestimated as the nets would be typically sampled during higher production times. In contrast, sediment traps are deployed over six months or more (Figure S1) thereby capturing seasonal variation. Sediment traps were deployed at different depths, typically over 1000 m and thereby deeper than our surface layer. We assume that sediment trap depth has negligible impact on foraminifera export because foraminifer tests sink relatively fast due to large size (Takahashi and Be, 1984; Caromel et al., 2014). We did not consider any biomass/export changes between the pre-industrial (the model) and current climate (plankton net and sediment trap), as these data are collected over wide time range (1970s-2010s) with changing climatologies.

6.3.3 Seasonality

To complement the annual comparison, we analysed the modelled seasonal pattern by finding each group's first month with peaking production. We also provided a comparison with plankton net and sediment trap data for most sampled locations in the Supplementary Material. We did not attempt to calculate a M-score for seasonal model-data comparisons because (1) the temporal coverage of observations is too low at most locations, and (2) the number of available locations is insufficient, creating large spatial bias towards specific oversampled locations.

6.4 Model performance metrics

We used the Mielke measure, or M-score (Watterson, 1996; Watterson et al., 2014), to quantify the model-data fit in (1) relative abundance and (2) annual average biomass/carbon export (Eqn. 21). This metric is a non-dimensional transformed mean square error combined mean and variance information (Gregoire et al., 2011; Hemer and Trenham, 2016). The score spans from -1 (low performance) to 1 (high performance) with 0 representing no predictive skill, and negative values representing negative correlation.

$$M = \frac{2}{\pi} arcsin \left[\frac{\sum_{i=1}^{n}(M_i - O_i)^2 / n}{\sigma_m^2 + \sigma_o^2 + (\mu_m - \mu_o)^2} \right]$$

(21)

The numerator corresponds to the mean square error, with M_i and O_i the model and observational value in the ith grid point, and n the total number of grid points. σ^2 and μ are the variance and mean, with superscripts m and o representing model and observed fields, respectively.

6.5 Global sensitivity analysis

We conduct a global sensitivity analysis (GSA) to explore the model robustness of our 1,200 experiments using the PAWN method (Pianosi and Wagener, 2015). This method measures the sensitivity of model outputs (focusing on M-score here) to different values of 12 input parameters (shown in Table 2). A total M-score is calculated by summing scores of each foraminifer group in biomass, POC export, and relative abundance (i.e., the total score ranges from -12 to 12). To further measure the uncertainty and robustness of the GSA results, we also apply a bootstrapping method with 1,000 resamples. This approach enables us to understand the confidence intervals of the sensitivity indices without running more experiments (Wagener and Pianosi, 2019). We bootstrapped our data using the *rsample* package (Silge et al., 2021) in the R software environment v4.1 (R Core Team, 2021).

7 Model results

7.1 Model ensemble results

The 1,200-member ensemble shows the ability to reproduce the observed POC export and relative abundance in terms of spatial pattern and values (both with highest total M-score > 1.0) but struggles with capturing the observed biomass (total M-score <0.5) (Figure 2). The M-score heatmap (Figure 2) shows the model runs cluster into 4 groups when compared to the three observational datasets. Cluster C, covering most parameter combinations, has an overall low performance in predicting foraminifer metrics. Cluster D shows an inverse abundance distribution compared to the observation. Cluster B only predicts POC export. Cluster A achieves the highest (i.e., the best) relative-abundance M-score with good predictions for biomass and POC export. Cluster A is also the only cluster with low foraminifer export, suggesting that low export is associated with parameter values required to have a high total M-score. The sensitivity analysis confirms this, as model performance is sensitive to those parameters controlling the source/sink of foraminifer export: symbiont size (ψ), autotrophy efficiency (λ_s), and palatability reduction (P_p) (Figure 3). Models with low export production and higher M-scores tend to have smaller foraminifera size and symbiont-to-host size ratio (for symbiotic groups) that facilitates foraminifera to survive in the low-

nutrient regions like subtropical gyres. These runs in cluster A also tend to have less than 20% decreased palatability caused by the shell and a high respiration cost, driving low biomass and export (Figure S2). In contrast, the runs with negative scoring (Cluster D) have larger foraminiferal size and higher protection against grazing (Figure S3). These results suggest that foraminifer body size and the calcification trait have a crucial role in foraminiferal distributions to achieve a match to the observed data. Questions addressing the size trait in more detail, like life history and geographic size distribution (Schmidt et al., 2004b), cannot be answered with this model ensemble as all foraminifer groups are assigned the same narrow cell size per run, even though they vary between runs.

We selected the model with parameter set (Table 2) that leads to the highest total M-score score (Table 3), hereafter termed the optimal model. This optimal model also has the highest M-score for the relative abundance (group mean = 0.3), for each group (Figure S5) and POC export (group mean = 0.16; Figure S4). More details are discussed in the next sections.

405
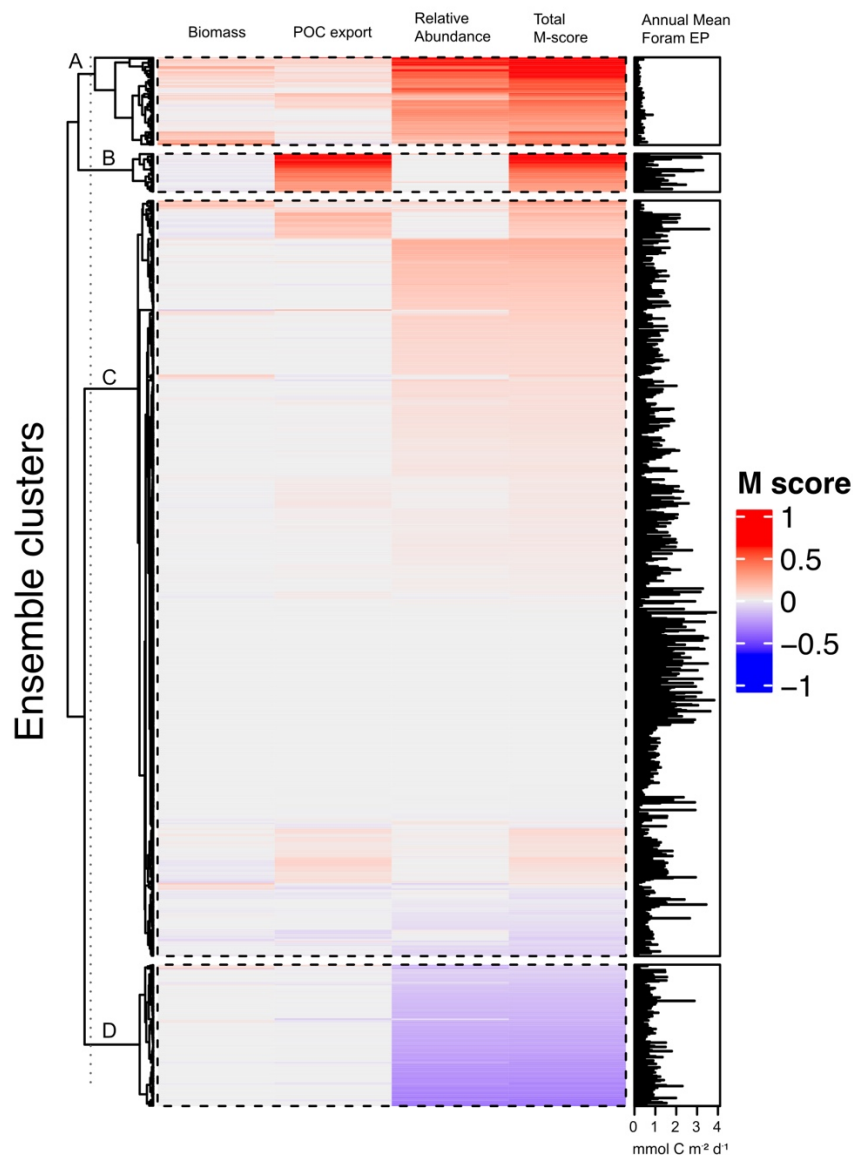
Figure 2. Foraminifera M-score heatmap of the model ensemble for foraminifera biomass (plankton net data), POC export (sediment trap data), Relative Abundance (sediment core top data). Each of first three columns shows the M-score sum of the four foraminifer groups, and the fourth column shows the sum of all the left three columns. The right panel shows the global annual mean export production of all foraminifer groups. The ensemble cluster was

410 **derived from a complete linkage clustering algorithm (Jarman, 2020). Higher M-scores have a better performance against observations, whilst negative values stand for negative correlation.**
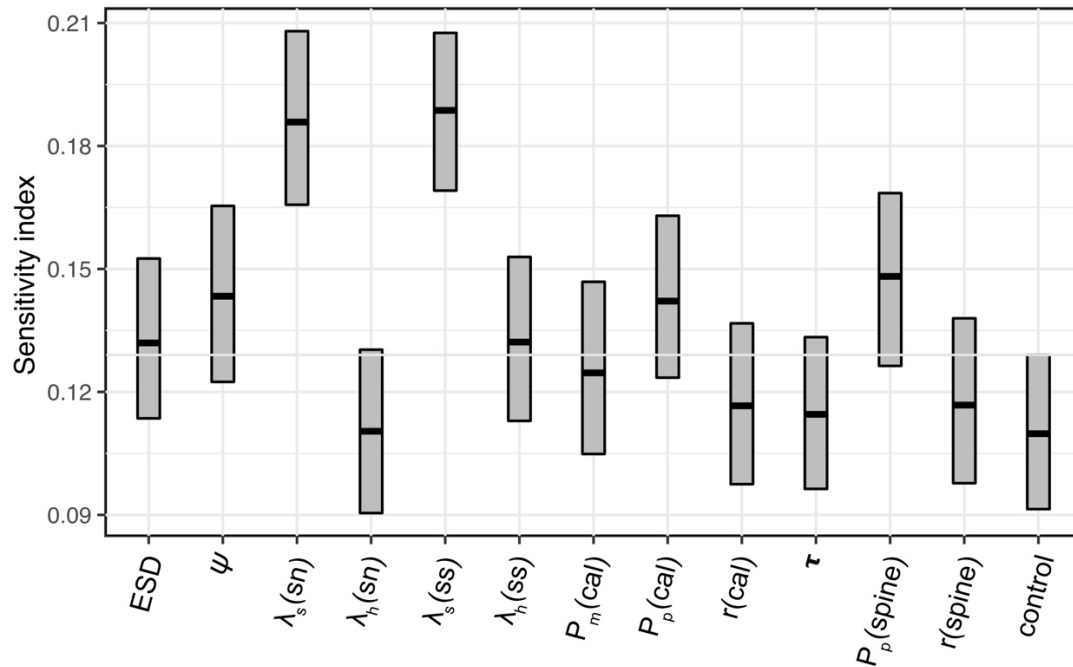
Figure 3. Model parameter sensitivity for overall model performance (summed M-scores). Bar boundaries indicate the 95-percent confidence interval with the thick line showing the mean value. The grey line indicates non-influential upper limit of index value as control group. sn, symbiont-facultative non-spinose; ss, symbiont-bearing spinose. cal, the abbreviation of calcification. τ is the spine effect on grazing rate.

Table 3. M-score values across foraminiferal groups for the optimal parameter set. The total foraminifera M-score is the sum of the M-scores of the 4 functional groups.

Groups	M-scores				
	Symbiont-barren non-spinose	Symbiont-barren spinose	Symbiont-facultative non-spinose	Symbiont-obligate spinose	Total foraminifera
Biomass	0.19	0.08	-0.05	-0.05	0.17
POC Export	0.11	0.07	0.43	0.02	0.63
Relative Abundance	0.51	0.35	0.02	0.32	1.20
Row sum	0.81	0.50	0.40	0.29	2.00

7.2 Relative abundance distribution of foraminifer groups

425 Our optimal model run compares generally well with the core-top data showing the relative spatial distribution of the four foraminifera functional groups (Figure 4; Table 3). The model agrees with the presence/absence of most groups in the sediment trap and plankton net studies (Figures 5 and 6). The model suggests that the symbiont-obligate spinose group is the most abundant with a global abundance of 60.7% (Figure 4g), dominating the tropical open oceans. In contrast, the symbiont-barren non-spinose (Figure 4a) and spinose groups (Figure 4c) dominate in the mid-to-high latitudes, contributing

430 25.5% and 9.4% of the global foraminifera abundance, respectively (note the symbiont-barren spinose type contains a small number of taxa with a relatively high contribution to the abundance). The model underestimates the symbiont-facultative group (Figure 4e) with visible model-data disparities in the eastern equatorial pacific where the sediment data show high abundance. This discrepancy may be due to the resistance to dissolution of some species (e.g., *N. dutertrei*) in high productivity settings as suggested in a previous model study (Lombard et al., 2011). Importantly though, it is not very clear

435 what triggers the presence or absence of symbionts, why this relationship changes and often the taxa are less well studied. That the summed abundances of these two symbiotic groups agree with the observations points to the ability of the facultatively symbiont bearing group to exploit the same benefits as the obligate symbiont bearing one. It also highlights our need to better understand how often symbiosis is used by the former group and what triggers the switch to the loss of symbionts.

440 Overall, the modelled Root Mean Square Error (RMSE) of relative abundance varies between 12% and 42% (Table S5). This result is comparable to the previous species-based models, like FORAMCLIM (5-23%, Lombard et al., 2011) and PLAFOM (22-25%, Fraile et al., 2009), which rely on well-established foraminifera species observations. Our results affirm that symbionts and spines and their assumed trade-offs are sufficient to explain significant parts of the relative abundance's geographic distribution. The distribution of non-symbiotic foraminifer in the model follows the biogeography of the prey

445 abundance with high numbers in high-nutrient areas (Figure S6). In contrast, symbiotic foraminifera grow in low-nutrient areas, because they have small-size symbionts with high nutrient affinities. The model underestimates symbiont-barren spinose foraminifera (mainly *G. bulloides*) in the Arabian Sea and South China Sea (Figure 4bd) probably because the model does not include their carnivorous feeding strategy.
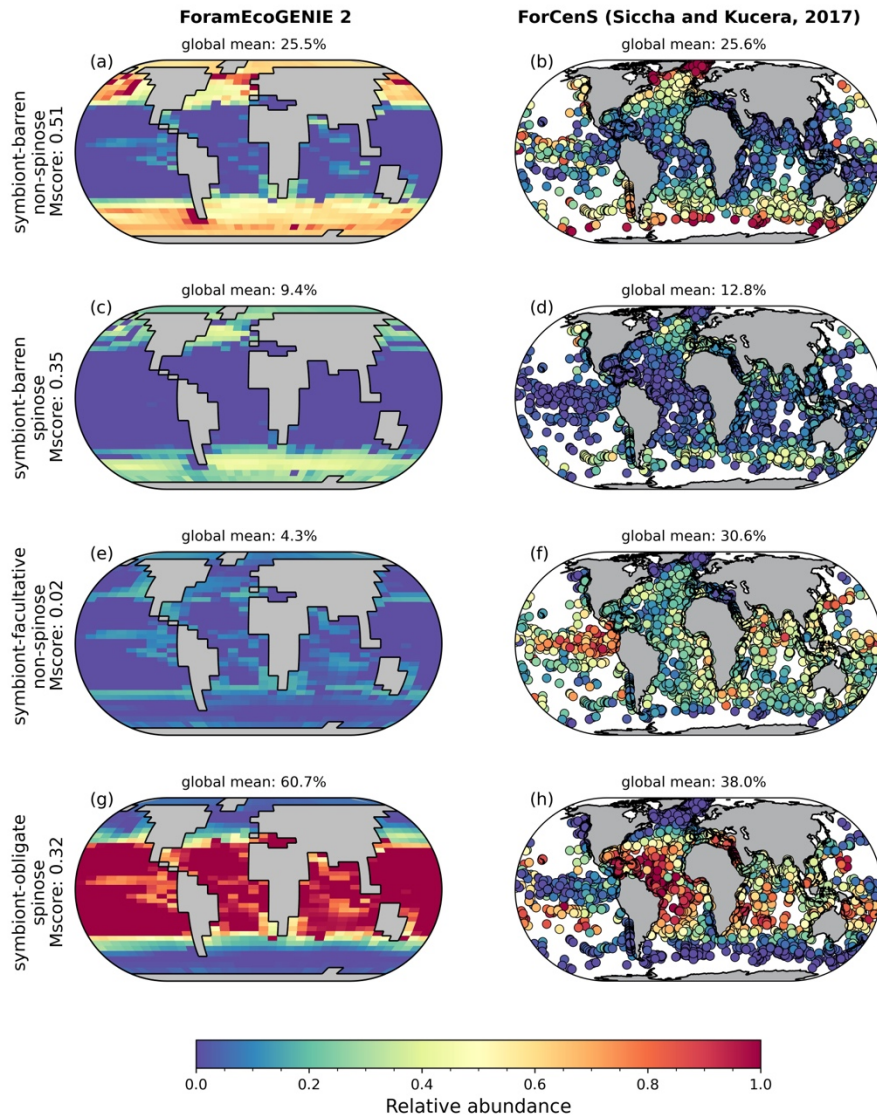
Figure 4. Relative abundance of the modelled (left column) four planktic foraminifer function groups, compared to the ForCenS sediment core-top dataset (right column; Siccha and Kucera, 2017). Subplot titles show the M-scores derived relative to observations and the global mean of relative abundance.

7.3 Annual average biomass of foraminifera groups

The model reproduces low biomass in planktic foraminifer in agreement with the plankton net data (Figure 5). The global annual mean biomass ranges from 0.001 to 0.010 mmol C m^{-3} equivalent to 0.08-0.8 mmol C m^{-2}, with the largest contribution from the symbiont-barren non-spinose group (Figure 7). Integrating across all groups, the model estimates a

global foraminifera biomass of 6.83 Tg C (Figure 7). Our annual mean biomass estimate is within the MAREDAT project result (0.24-0.94 mmol C m^{-2}) (Schiebel and Movellan, 2012).

460 The optimal model M-score is low for biomass when compared to the plankton net tow (<0.2; Table 3), possibly because of the low data coverage and the previously mentioned intrinsic seasonal bias in the data compared to annual averages. Our ensemble resulted in higher M-scores for biomass, but at the cost of a lower M-score for relative-abundance and export.
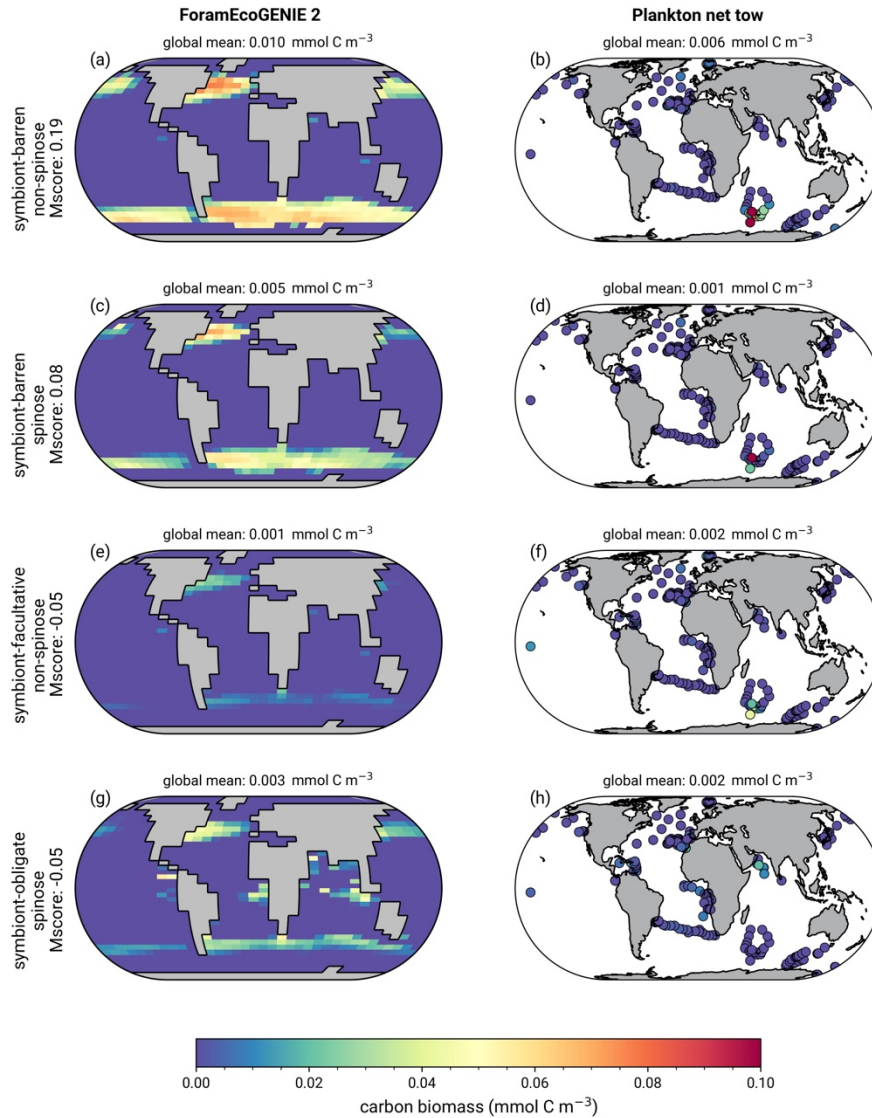
Figure 5. ForamEcoGEnIE 2.0 annual average foraminifera biomass (mmol C m^{-3}) compared with plankton net data
465 **(right column) for the four main functional groups of planktic foraminifera.**

7.4 Annual average POC and calcite export of foraminifera groups

The model reproduces consistent distributions and magnitude of POC export compared to sediment trap data for all four groups (Figures 6 and 7). The model estimates a POC export of 0.002-0.031 mmol C m^{-2} d^{-1}, which agrees well with 0.001-0.026 mmol C m^{-2} d^{-1} for the sediment trap data, despite a medium total M-score for the model POC export (0.63) likely caused by the limited geographic coverage akin to the biomass comparison.

Globally, the model suggests a foraminifer-derived organic carbon export of 0.1 Gt C yr^{-1}, dominated by the symbiont-barren non-spinose group (55%), followed by the symbiont-barren spinose, symbiont-facultative and symbiont-obligate groups (30%, 3% and 11%, respectively). Integrating across the ecogroups and using the empirically averaged PIC:POC ratio of 0.36 (Schiebel and Movellan, 2012), our model estimates a total calcite flux of pelagic foraminifera of 0.033 Gt PIC yr^{-1} (Figure 8). This model estimate is at least five times smaller than Schiebel (2002)'s estimate of 0.16–0.39 Gt PIC yr^{-1} (for the top 100 –m). There are a number of possible reasons for this: 1) a field site selection bias to avoid regions which are very low abundance, 2) our calibration of modelled surface export with deep sediment traps data characterised by typically lower export (as deployed at about 2 km depth), and 3) the temporal variability of observation which is not well captured in the model.
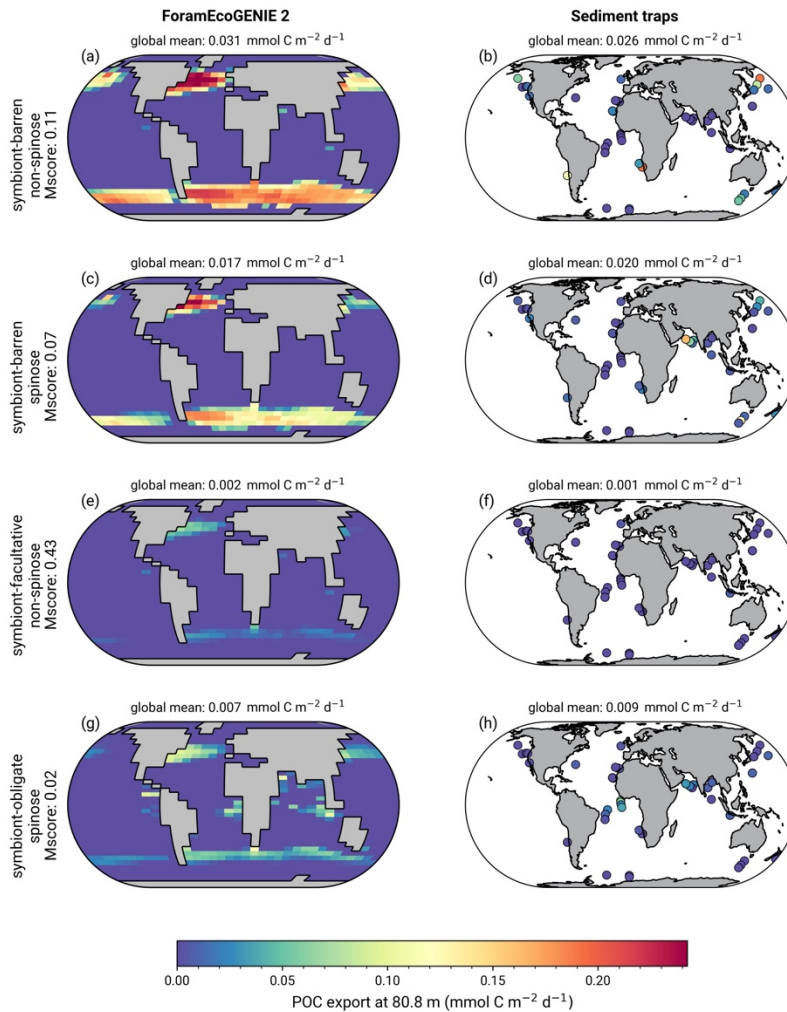
Figure 6. ForamEcoGEnIE 2.0 foraminifera annual average POC export (mmol C m^{-2} d^{-1}) below the euphotic zone (80.8 m) in comparison to sediment trap samples (right column).
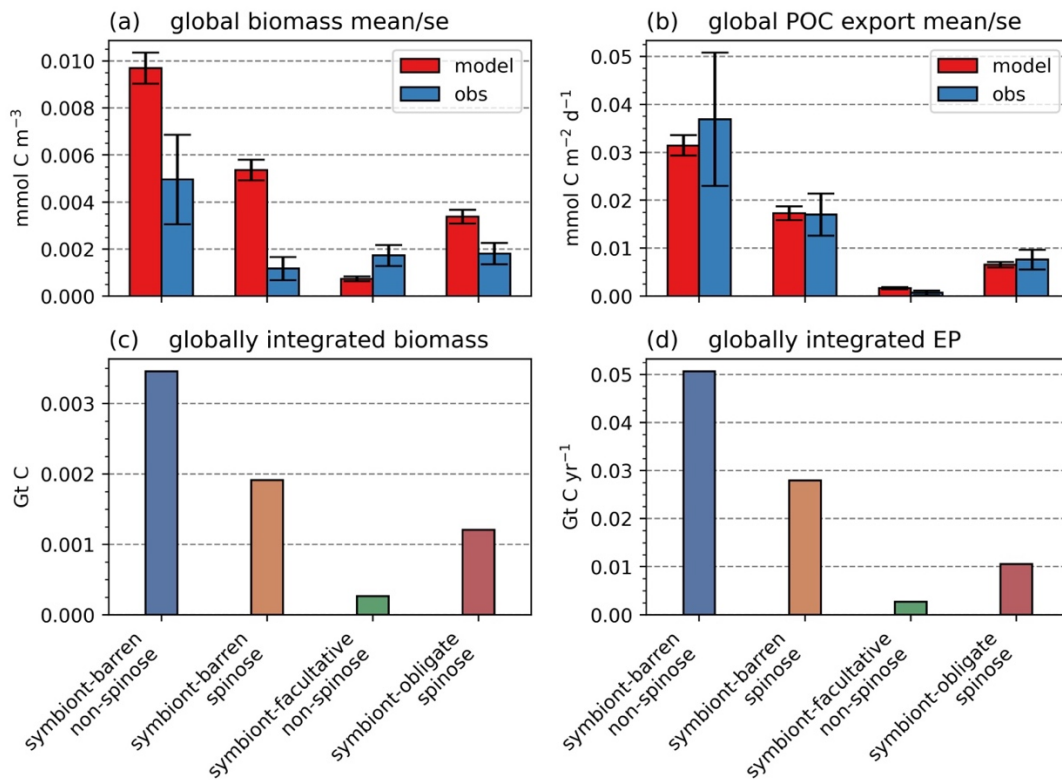
485

Figure 7. Global ForamEcoGEnIE 2.0 annual average biomass and POC export produced by the four foraminifer groups: (a) modelled (red) and observational (blue) biomass (mmol C m^{-3}); (b) POC export below the euphotic zone (mmol C m^{-3} d^{-1}). Bar height and error bar represents the spatial mean value and standard error, respectively. Panels c and d show the globally integrated model estimates for (c) carbon biomass (Gt C) and (d) export production (EP, Gt C yr^{-1}).

490
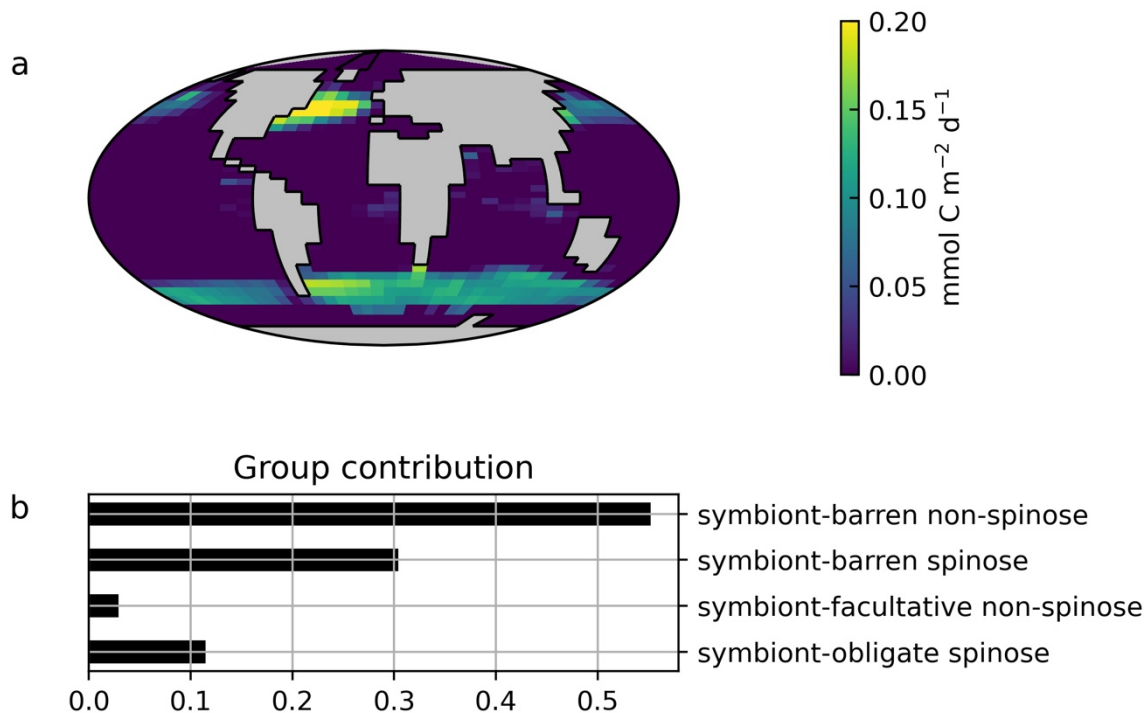
Figure 8. Global ForamEcoGEnIE 2.0 estimates for (a) surface foraminiferal calcite flux (at 80.8 m; mmol C m^{-2} yr^{-1})
495 and (b) group's contribution.

7.5 Seasonal variations of foraminifera biomass and POC export

Our model shows the different seasonal pattern for each foraminifer group (Figure 9), generally consistent with sediment trap study (Jonkers and Kučera, 2015). Jonkers and Kučera (2015) divide the foraminiferal assemblages into a warm group
500 (representing the symbiont-bearing group), cool and temperate group (representing the two symbiont-barren groups), and deep dwelling group according to their seasonal cycle patterns. The cool/temperate group has bloom in spring or summer (Figure 9a), while the warm group in tropical oceans shows weak and random seasonality (Figure 9d). The model also captures the earlier-when-warmer signature in the cool/temperate group, i.e., the peaking time is strongly coupled to temperature gradient from high to low latitude (Figure 9a).

505 The model generally underestimates seasonal amplitudes of export production (Figure S7). Plankton net data cannot be compared seasonally due to the very short nature of data collection, despite the general agreement (Figure S8). The low model export production is not unique to our model and also evident in PLAFOM 2.0 (Kretschmer et al., 2018). Intra-annual variabilities in abundance are driven by the seasonal environmental changes which determine how optimal foraminifera are in the ecological niche. While temperature is often assumed as the primary driver for foraminiferal ecology (Schmidt et al.,
510 2004b; Be and Hamlin, 1967), many other parameters such as primary productivity are correlated with temperature and

hence difficult to separate their effects (Jonkers and Kučera, 2015). We suggest that additional functional trait data collections assessing temporal variability, increased geographic coverage, information on deeper dwelling species and life history cycle will contribute to resolve this gap in the future.
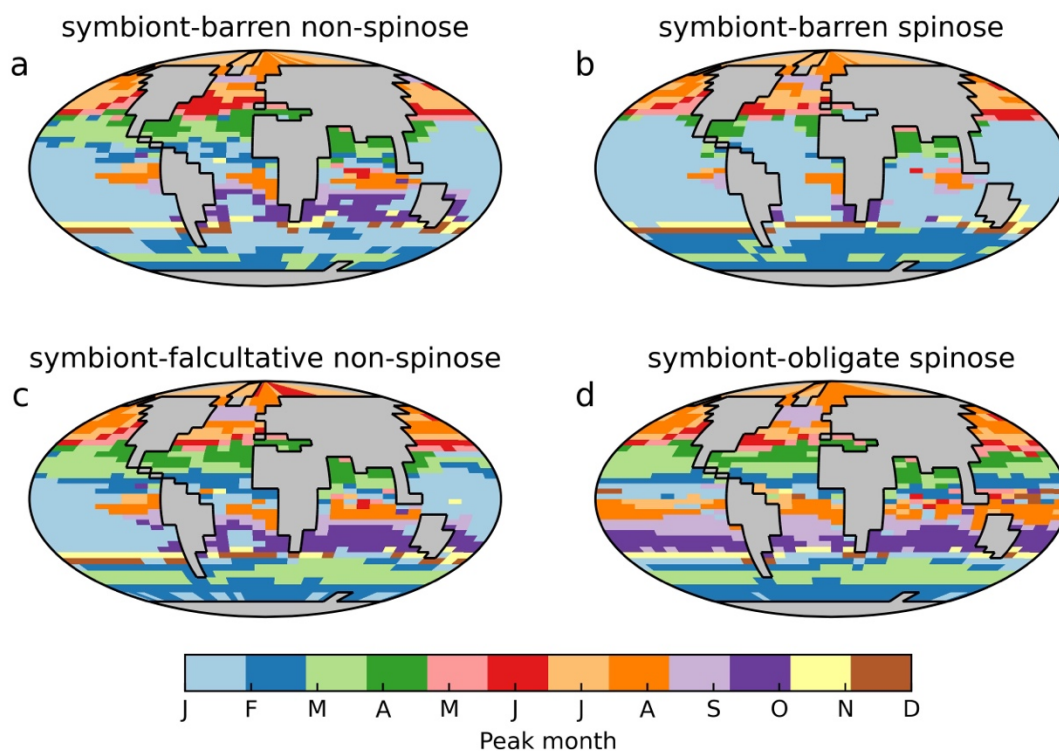
Figure 9. The peak month of modelled biomass annual time series of each foraminifer group in our best ForamEcoGEnIE 2.0 run. Note the months in Southern Hemisphere indicate the opposite seasonality of North Hemisphere.

520 ## 8 Comparison to prior model iterations

By comparing ForamEcoGEnIE 2.0 with EcoGEnIE (Ward et al., 2018) and ForamEcoGEnIE 1.0 (Grigoratou et al., 2021a), we find that adding foraminifera groups increases the total-plankton mean body size in the tropical and subtropical regions by roughly 20% due larger size of foraminifera (modelled as 190 μm, Figure 10c). At the same time, the new iteration decreases the plankton mean size in subpolar areas (< 10%) due to additional grazing pressure by foraminifers on the

525 plankton. In contrast, the total-plankton biomass stays almost the same between the model versions because of the low standing stocks of foraminifers. Net primary productivity (NPP) and POC export also do not change, apart from a small drop in the subpolar regions due to enhanced foraminifera grazing. Therefore, ForamEcoGEnIE 2.0 performs as well as the

previous version in terms of total plankton size, biomass, carbon export and NPP, while capturing foraminifera diversity and biogeography.

530   While ForamEcoGEnIE 2.0 developments focused on improving diversity in plankton ecology, it also lays the foundation for future studies on the ocean carbon cycle under different climates, past or the future. For example, the inclusion of spinose foraminifera is important for particle sinking as they produce and export more calcite than their non-spinose counterpart (Takahashi and Be, 1984). It also opens the door for studies of past climates by expanding the foraminifer global niche, which may influence the ocean carbon cycles by changing the locations of calcite export and distribution of surface

535   alkalinity. So far, no Earth system model has included foraminifer groups acting on the carbon cycle, which would be important avenue for future research.
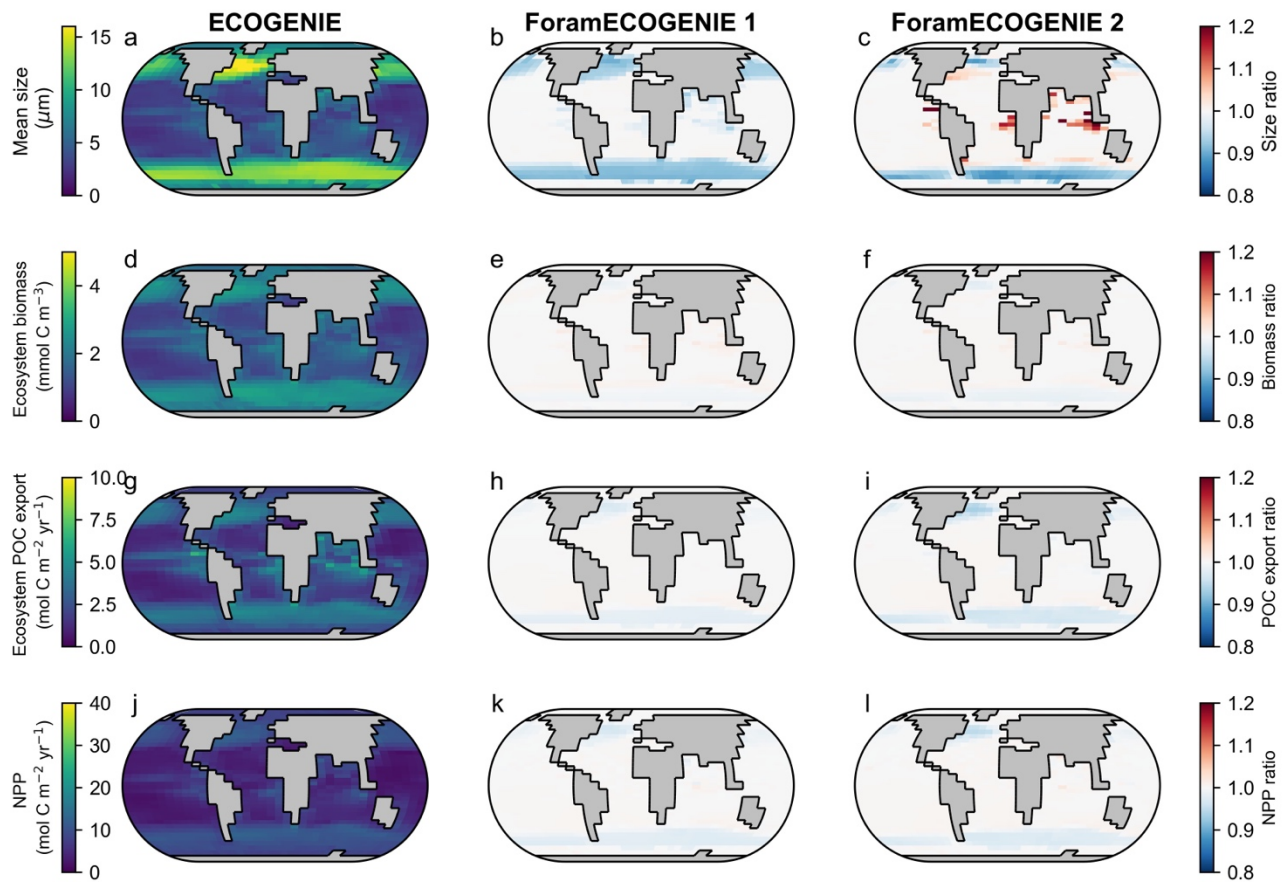
Figure 10. Comparison of the tuned ForamEcoGEnIE 2.0 (third column, with four foraminifer groups) with EcoGEnIE (first column; Ward et al., 2018) and ForamEcoGEnIE 1.0 (second column, with non-spinose non-symbiont foraminifer only; Grigoratou et al., 2021a) for (a-c) total plankton mean size, (d-f) total plankton biomass,

(g-i) total POC export, and (j-l) Net Primary Production (NPP). The first column displays absolute values, whilst the latter two show the ratio relative to the first column.

9 Model limitation

545 While making explicit progress in including planktic foraminifers into a modelling framework with a range of traits, ForamEcoGEnIE 2.0 is limited by the non-explicit implementations of spines and symbiosis. Currently, our model represents symbiosis based on mixotrophy implementation. According to the definition of mixotrophy types in Mitra et al. (2016), our modelling approach falls within constitutive (inherent or innate) mixotroph rather than the non-constitutive mixotroph grouping. Such indirect photosymbiotic relationships in the model might miss any differential climate sensitivities of

550 symbiont and host. Furthermore, the current parameterization of calcification, spines and symbiosis will not respond directly to environmental changes, such as bleaching at high temperatures (Edgar et al., 2013) or reduced weight under high CO_2 (Barker and Elderfield, 2002). However, relying on parameterisation is common in EMICs (Claussen et al., 2002), as quantitative experimental studies are lacking now to define the trade-offs and benefits. This lack of understanding of trade-off and their change during development makes it also currently impossible to model the life cycle, though further

555 development would be the inclusion of size classes other than 190µm.

Some potentially important trait interactions and physiological variation are not included in the model. For example, the model assumes that the spine and symbiosis are independent. However, observations suggest that foraminifera symbionts are placed along spines during daytime (LeKieffre et al., 2018), increasing the efficiency of the symbiont's photosynthesis due to a higher surface area relative to non-spinose species by avoiding shading.

560

10 Ecosystem model implementation and complexity

Current coupled Earth system and ecosystem models mostly rely on Nutrient-Plankton-Zooplankton-Detritus (NPZD) (Keller et al., 2012; Watanabe et al., 2011) or Plankton Functional Type (PFT) (Moore et al., 2001; Aumont et al., 2015) approaches. NPZD models focus on biogeochemical fluxes and ignore diversity of phytoplankton and zooplankton. In

565 contrast, PFT models explicitly represent plankton functional types (e.g., diatoms, coccolithophores) and size classes (e.g., picoplankton, nanoplankton, microplankton), improving performance in reconstructing observed pattern like chl *a* (Quéré et al., 2005) or peak production in oligotrophic areas (Tréguer et al., 2018). Additional traits beyond size, like symbiosis (Suggett et al., 2017) or body extension (Ohman, 2019), play an important role in determining plankton feeding, metabolism and export efficiency, but are often missing in the current generation of coupled models. Trait-based models, such as Darwin

570 (Follows et al., 2007) and EcoGEnIE (Ward et al., 2018), resolve higher plankton diversity by linking key traits with trade-offs (e.g. the allometric relationships for size), allowing more continuous representation based on physiology (Follows and Dutkiewicz, 2011). This approach enables to include non-culturable species or species with limited laboratory data. Uniquely, this modelling approach also allows to characterise extinct taxa and past geological records with different physiologies and niches.

575

There is still a debate on whether higher ecosystem complexity is needed (Anderson, 2005; Quéré et al., 2005) as more parameters introduce more freedom andlonger run time. However, recent studies highlight the importance of biodiversity in the marine biological pumps (Tréguer et al., 2018). The presence of functional group like diazotroph can alter the response of primary productivity to global warming (Bopp et al., 2022). Therefore, compared to the simple food web structure in

580   current models, ecosystem implementation very likely to improve future prediction of biological carbon pump and carbon cycle (Wilson et al., 2022) building on novel additions in models of ecosystem complexities such as more functional types, variable stoichiometry, and nutrient co-limitations (Séférian et al., 2020).

11 Summary

585   In this study, we extended the trait-based planktic foraminifer model, ForamEcoGEnIE, to include symbiosis and spine traits and thereby resolve all main foraminifer functional groups. Using Latin Hypercube Sampling, we generated 1,200 parameter samples and compared these with three global observational sources: sediment surface core-top, plankton nets, and sediment traps. We assessed the model performance describing biogeographic distributions, and quantifying carbon biomass and foraminifer-derived carbon export. Our global sensitivity analysis shows the symbiosis and the palatability reduction due to

590   the spinose test strongly influences model performance. Our best set of model parameters successfully reproduces the modern biogeographical distribution of the four foraminifera ecogroups and produces a global annual mean biomass (0.001 to 0.010 mmol C m^{-3}) and foraminifer-derived organic carbon export (0.002-0.031 mmol C m^{-2} d^{-1}) close to observations. The two symbiont-barren groups account for 85% of standing stocks and foraminifer-derived carbon export. The model accurately reproduces peak time of seasonal time-series observations of foraminiferal biomass and organic carbon flux but

595   performs poorer in seasonal amplitudes, particularly in upwelling regions. These results provide confidence in the model's ability to explore foraminifer ecology and diversity in the geological record, for example of the last glacial maximum, as well as helping to solve riddles about their ecology in the past. The trait-based framework of cGEnIE ecosystem provides the potential to extend the model by presenting more traits such as life history and differential calcification rates across groups.

600   **Code and data availability**

The source codes and data are archived in https: doi.org/10.5281/zenodo.6808760. Experiment configuration and observational dataset can be found in genie-userconfig/MS/yingetal.GMD.2022. A general manual for cGEnIE model can be found in https://github.com/derpycode/muffindoc.

605   **Author contribution**

RY, FMM, JDW, DNS designed the study. RY, FMM, JDW developed the model code. RY performed the experiments, data collection and visualisation. All authors interpreted the data and wrote and edited the original draft.

Competing interests

610   The authors declare that they have no conflict of interest.

Acknowledgements

We thank two anonymous reviewers for their helpful and constructive comments. We acknowledge funding from NERC (NE/P019439/1 for DNS and JDW), NE/N011708/1 (FMM), TMS Angelina Messina Grant (RY), China Scholarship

615   Council (RY, No. 202006380070), and AXA Research Fund Postdoctoral Fellowship (JDW). We would like to thank Maria Grigoratou for her insights on the model development and Ruby Barrett for the proof reading.

References

Adloff, M., Ridgwell, A., Monteiro, F. M., Parkinson, I. J., Dickson, A. J., Pogge von Strandmann, P. A. E., Fantle, M. S.,
620   and Greene, S. E.: Inclusion of a suite of weathering tracers in the cGENIE Earth system model – muffin release v.0.9.23, Geosci. Model Dev., 14, 4187–4223, https://doi.org/10.5194/gmd-14-4187-2021, 2021.

Andersen, K. H., Berge, T., Gonçalves, R. J., Hartvig, M., Heuschele, J., Hylander, S., Jacobsen, N. S., Lindemann, C., Martens, E. A., Neuheimer, A. B., Olsson, K., Palacz, A., Prowe, A. E. F., Sainmont, J., Traving, S. J., Visser, A. W., Wadhwa, N., and Kiørboe, T.: Characteristic Sizes of Life in the Oceans, from Bacteria to Whales, Annual Review of
625   Marine Science, 8, 217–241, https://doi.org/10/f3pdzr, 2016.

Anderson, O. R. and Bé, A. W. H.: The ultrastructure of a planktonic foraminifer, Globigerinoides sacculifer (Brady), and its symbiotic dinoflagellates, Journal of Foraminiferal Research, 6, 1–21, https://doi.org/10.2113/gsjfr.6.1.1, 1976.

Anderson, O. R., Spindler, M., Bé, A. W. H., and Hemleben, Ch.: Trophic activity of planktonic foraminifera, J. Mar. Biol. Ass., 59, 791–799, https://doi.org/10.1017/S002531540004577X, 1979.

630   Anderson, R. P.: When and how should biotic interactions be considered in models of species niches and distributions?, Journal of Biogeography, 44, 8–17, https://doi.org/10.1111/jbi.12825, 2017.

Anderson, T. R.: Plankton functional type modelling: running before we can walk?, Journal of Plankton Research, 27, 1073–1081, https://doi.org/10.1093/plankt/fbi076, 2005.

Aumont, O., Ethé, C., Tagliabue, A., Bopp, L., and Gehlen, M.: PISCES-v2: an ocean biogeochemical model for carbon and
635   ecosystem studies, Geoscientific Model Development, 8, 2465–2513, https://doi.org/10.5194/gmd-8-2465-2015, 2015.

Aze, T., Ezard, T. H. G., Purvis, A., Coxall, H. K., Stewart, D. R. M., Wade, B. S., and Pearson, P. N.: A phylogeny of Cenozoic macroperforate planktonic foraminifera from fossil data, Biological Reviews, 86, 900–927, https://doi.org/10/dvjwx6, 2011.

Barker, S. and Elderfield, H.: Foraminiferal Calcification Response to Glacial-Interglacial Changes in Atmospheric CO2,
640   Science, 297, 833–836, https://doi.org/10.1126/science.1072815, 2002.

Be, A. W. H. and Hamlin, W. H.: Ecology of Recent Planktonic Foraminifera: Part 3: Distribution in the North Atlantic during the Summer of 1962, Micropaleontology, 13, 87, https://doi.org/10/b99v5t, 1967.

Bé, A. W. H., Spero, H. J., and Anderson, O. R.: Effects of symbiont elimination and reinfection on the life processes of the planktonic foraminifer Globigerinoides sacculifer, Mar. Biol., 70, 73–86, https://doi.org/10.1007/BF00397298, 1982.

645   Bec, Bé., Collos, Y., Vaquer, A., Mouillot, D., and Souchu, P.: Growth rate peaks at intermediate cell size in marine photosynthetic picoeukaryotes, Limnol. Oceanogr., 53, 863–867, https://doi.org/10.4319/lo.2008.53.2.0863, 2008.

Bopp, L., Aumont, O., Kwiatkowski, L., Clerc, C., Dupont, L., Ethé, C., Gorgues, T., Séférian, R., and Tagliabue, A.: Diazotrophy as a key driver of the response of marine net primary productivity to climate change, Biogeosciences, 19, 4267–4285, https://doi.org/10.5194/bg-19-4267-2022, 2022.

650   Brovkin, V., Brücher, T., Kleinen, T., Zaehle, S., Joos, F., Roth, R., Spahni, R., Schmitt, J., Fischer, H., Leuenberger, M., Stone, E. J., Ridgwell, A., Chappellaz, J., Kehrwald, N., Barbante, C., Blunier, T., and Dahl Jensen, D.: Comparative carbon cycle dynamics of the present and last interglacial, Quaternary Science Reviews, 137, 15–32, https://doi.org/10.1016/j.quascirev.2016.01.028, 2016.

Brown, J. H., Gillooly, J. F., Allen, A. P., Savage, V. M., and West, G. B.: Toward a Metabolic Theory of Ecology, Ecology,
655   1771–1789, https://doi.org/10.1890/03-9000@10.1002/(ISSN)1939-9170.MacArthurAward, 2004.

Buckley, L. B., Urban, M. C., Angilletta, M. J., Crozier, L. G., Rissler, L. J., and Sears, M. W.: Can mechanism inform species' distribution models?, Ecology Letters, 13, 1041–1054, https://doi.org/10.1111/j.1461-0248.2010.01479.x, 2010.

Buitenhuis, E. T., Vogt, M., Moriarty, R., Bednaršek, N., Doney, S. C., Leblanc, K., Le Quéré, C., Luo, Y.-W., O'Brien, C., O'Brien, T., Peloquin, J., Schiebel, R., and Swan, C.: MAREDAT: towards a world atlas of MARine Ecosystem DATa,
660   Earth System Science Data, 5, 227–239, https://doi.org/10.5194/essd-5-227-2013, 2013.

Buitenhuis, E. T., Quéré, C. L., Bednaršek, N., and Schiebel, R.: Large Contribution of Pteropods to Shallow CaCO3 Export, Global Biogeochemical Cycles, 33, 458–468, https://doi.org/10/gjpnzt, 2019.

Cao, L., Eby, M., Ridgwell, A., Caldeira, K., Archer, D., Ishida, A., Joos, F., Matsumoto, K., Mikolajewicz, U., Mouchet, A., Orr, J. C., Plattner, G.-K., Schlitzer, R., Tokos, K., Totterdell, I., Tschumi, T., Yamanaka, Y., and Yool, A.: The role of
665   ocean transport in the uptake of anthropogenic CO2, Biogeosciences, 6, 375–390, https://doi.org/10/fp96kf, 2009.

Caromel, A. G. M., Schmidt, D. N., Phillips, J. C., and Rayfield, E. J.: Hydrodynamic constraints on the evolution and ecology of planktic foraminifera, Marine Micropaleontology, 106, 69–78, https://doi.org/10.1016/j.marmicro.2014.01.002, 2014.

Castellani, M., Våge, S., Strand, E., Thingstad, T. F., and Giske, J.: The Scaled Subspaces Method: A new trait-based
670   approach to model communities of populations with largely inhomogeneous density, Ecological Modelling, 251, 173–186, https://doi.org/10.1016/j.ecolmodel.2012.12.006, 2013.

Claussen, M., Mysak, L., Weaver, A., Crucifix, M., Fichefet, T., Loutre, M.-F., Weber, S., Alcamo, J., Alexeev, V., Berger, A., Calov, R., Ganopolski, A., Goosse, H., Lohmann, G., Lunkeit, F., Mokhov, I., Petoukhov, V., Stone, P., and Wang, Z.: Earth system models of intermediate complexity: closing the gap in the spectrum of climate system models, Climate
675   Dynamics, 18, 579–586, https://doi.org/10.1007/s00382-001-0200-1, 2002.

Daniels, C. J., Poulton, A. J., Balch, W. M., Marañón, E., Adey, T., Bowler, B. C., Cermeño, P., Charalampopoulou, A., Crawford, D. W., Drapeau, D., Feng, Y., Fernández, A., Fernández, E., Fragoso, G. M., González, N., Graziano, L. M., Heslop, R., Holligan, P. M., Hopkins, J., Huete-Ortega, M., Hutchins, D. A., Lam, P. J., Lipsen, M. S., López-Sandoval, D. C., Loucaides, S., Marchetti, A., Mayers, K. M. J., Rees, A. P., Sobrino, C., Tynan, E., and Tyrrell, T.: A global compilation

680   of coccolithophore calcification rates, Earth Syst. Sci. Data, 10, 1859–1876, https://doi.org/10.5194/essd-10-1859-2018, 2018.

Droop, M. R.: Vitamin B12 and Marine Ecology. IV. The Kinetics of Uptake, Growth and Inhibition in Monochrysis Lutheri, J. Mar. Biol. Ass., 48, 689–733, https://doi.org/10.1017/S0025315400019238, 1968.

Edgar, K. M., Bohaty, S. M., Gibbs, S. J., Sexton, P. F., Norris, R. D., and Wilson, P. A.: Symbiont 'bleaching' in planktic
685   foraminifera during the Middle Eocene Climatic Optimum, Geology, 41, 15–18, https://doi.org/10/f4jwbp, 2013.

Edwards, K. F., Thomas, M. K., Klausmeier, C. A., and Litchman, E.: Allometric scaling and taxonomic variation in nutrient utilization traits and maximum growth rate of phytoplankton, Limnol. Oceanogr., 57, 554–566, https://doi.org/10.4319/lo.2012.57.2.0554, 2012.

Edwards, N. R. and Marsh, R.: Uncertainties due to transport-parameter sensitivity in an efficient 3-D ocean-climate model,
690   Clim Dyn, 24, 415–433, https://doi.org/10/fcvq9k, 2005.

Ezard, T. H. G., Aze, T., Pearson, P. N., and Purvis, A.: Interplay Between Changing Climate and Species' Ecology Drives Macroevolutionary Dynamics, Science, 332, 349–351, https://doi.org/10/bd77gm, 2011.

Fiksen, Ø., Follows, M. J., and Aksnes, D. L.: Trait-based models of nutrient uptake in microbes extend the Michaelis-Menten framework, Limnol. Oceanogr., 58, 193–202, https://doi.org/10.4319/lo.2013.58.1.0193, 2013.

695   Fisher, R. A., Corbet, A. S., and Williams, C. B.: The Relation Between the Number of Species and the Number of Individuals in a Random Sample of an Animal Population, Journal of Animal Ecology, 12, 42–58, https://doi.org/10.2307/1411, 1943.

Flynn, K. J.: The importance of the form of the quota curve and control of non-limiting nutrient transport in phytoplankton models, Journal of Plankton Research, 30, 423–438, https://doi.org/10.1093/plankt/fbn007, 2008.

700   Follows, M. J. and Dutkiewicz, S.: Modeling Diverse Communities of Marine Microbes, Annu. Rev. Mar. Sci., 3, 427–451, https://doi.org/10/b3w27x, 2011.

Follows, M. J., Dutkiewicz, S., Grant, S., and Chisholm, S. W.: Emergent Biogeography of Microbial Communities in a Model Ocean, Science, 315, 1843–1846, https://doi.org/10/bf6j95, 2007.

Fraile, I., Schulz, M., Mulitza, S., and Kucera, M.: Predicting the global distribution of planktonic foraminifera using a
705   dynamic ecosystem model, Biogeosciences, 5, 891–911, https://doi.org/10/dkjgd3, 2008.

Fraile, I., Schulz, M., Mulitza, S., Merkel, U., Prange, M., and Paul, A.: Modeling the seasonal distribution of planktonic foraminifera during the Last Glacial Maximum, Paleoceanography, 24, https://doi.org/10/dh2z9t, 2009.

Gaskell, D. E., Ohman, M. D., and Hull, P. M.: Zooglider-Based Measurements of Planktonic Foraminifera in the California Current System, Journal of Foraminiferal Research, 49, 390–404, https://doi.org/10.2113/gsjfr.49.4.390, 2019.

710   Geider, R. J., Maclntyre, H. L., and Kana, T. M.: A dynamic regulatory model of phytoplanktonic acclimation to light, nutrients, and temperature, Limnol. Oceanogr., 43, 679–694, https://doi.org/10.4319/lo.1998.43.4.0679, 1998.

Gregoire, L. J., Valdes, P. J., Payne, A. J., and Kahana, R.: Optimal tuning of a GCM using modern and glacial constraints, Clim Dyn, 37, 705–719, https://doi.org/10.1007/s00382-010-0934-8, 2011.

Grigoratou, M., Monteiro, F. M., Schmidt, D. N., Wilson, J. D., Ward, B. A., and Ridgwell, A.: A trait-based modelling
715 approach to planktonic foraminifera ecology, Biogeosciences, 16, 1469–1492, https://doi.org/10/gj349g, 2019.

Grigoratou, M., Monteiro, F. M., Wilson, J. D., Ridgwell, A., and Schmidt, D. N.: Exploring the impact of climate change on
the global distribution of non-spinose planktonic foraminifera using a trait-based ecosystem model, Glob Change Biol,
gcb.15964, https://doi.org/10.1111/gcb.15964, 2021a.

Grigoratou, M., Monteiro, F. M., Ridgwell, A., and Schmidt, D. N.: Investigating the benefits and costs of spines and diet on
720 planktonic foraminifera distribution with a trait-based ecosystem model, Marine Micropaleontology, 102004,
https://doi.org/10/gkbn65, 2021b.

Hemer, M. A. and Trenham, C. E.: Evaluation of a CMIP5 derived dynamical global wind wave climate model ensemble,
Ocean Modelling, 103, 190–203, https://doi.org/10.1016/j.ocemod.2015.10.009, 2016.

Hemleben, C., Spindler, M., and Erson, O. R.: Modern planktonic foraminifera, 363 pp., 1989.

725 Henehan, M. J., Ridgwell, A., Thomas, E., Zhang, S., Alegret, L., Schmidt, D. N., Rae, J. W. B., Witts, J. D., Landman, N.
H., Greene, S. E., Huber, B. T., Super, J. R., Planavsky, N. J., and Hull, P. M.: Rapid ocean acidification and protracted
Earth system recovery followed the end-Cretaceous Chicxulub impact, PNAS, 116, 22500–22504, https://doi.org/10/ggbnrm,
2019.

Holling, C. S.: The Functional Response of Predators to Prey Density and its Role in Mimicry and Population Regulation,
730 Mem. Entomol. Soc. Can., 97, 5–60, https://doi.org/10/fhjtms, 1965.

Hönisch, B., Ridgwell, A., Schmidt, D. N., Thomas, E., Gibbs, S. J., Sluijs, A., Zeebe, R., Kump, L., Martindale, R. C.,
Greene, S. E., Kiessling, W., Ries, J., Zachos, J. C., Royer, D. L., Barker, S., Marchitto, T. M., Moyer, R., Pelejero, C.,
Ziveri, P., Foster, G. L., and Williams, B.: The Geological Record of Ocean Acidification, Science, 335, 1058–1063,
https://doi.org/10/gdj3zf, 2012.

735 Jarman, A. M.: Hierarchical cluster analysis: Comparison of single linkage, complete linkage, average linkage and centroid
linkage method, Georgia Southern University, 2020.

Jonkers, L. and Kučera, M.: Global analysis of seasonality in the shell flux of extant planktonic Foraminifera,
Biogeosciences, 12, 2207–2226, https://doi.org/10.5194/bg-12-2207-2015, 2015.

Keller, D. P., Oschlies, A., and Eby, M.: A new marine ecosystem model for the University of Victoria Earth System
740 Climate Model, Geoscientific Model Development, 5, 1195–1220, https://doi.org/10.5194/gmd-5-1195-2012, 2012.

Kiørboe, T., Visser, A., and Andersen, K. H.: A trait-based approach to ocean ecology, ICES Journal of Marine Science, 75,
1849–1863, https://doi.org/10.1093/icesjms/fsy090, 2018.

Kretschmer, K., Kucera, M., and Schulz, M.: Modeling the distribution and seasonality of Neogloboquadrina pachyderma in
the North Atlantic Ocean during Heinrich Stadial 1, Paleoceanography, 31, 986–1010,
745 https://doi.org/10.1002/2015PA002819, 2016.

Kretschmer, K., Jonkers, L., Kucera, M., and Schulz, M.: Modeling seasonal and vertical habitats of planktonic foraminifera
on a global scale, Biogeosciences, 15, 4405–4429, https://doi.org/10/gdx3bj, 2018.

Kucera, M. and Schonfeld, J.: The origin of modern oceanic foraminiferal faunas and Neogene climate change, in: Deep-
Time Perspectives on Climate Change: Marrying the Signal from Computer Models and Biological Proxies, edited by:

Williams, M., Haywood, A. M., Gregory, F. J., and Schmidt, D. N., The Geological Society of London on behalf of The Micropalaeontological Society, 409–425, https://doi.org/10.1144/TMS002.18, 2007.

LeKieffre, C., Spero, H. J., Russell, A. D., Fehrenbacher, J. S., Geslin, E., and Meibom, A.: Assimilation, translocation, and utilization of carbon between photosynthetic symbiotic dinoflagellates and their planktic foraminifera host, Mar Biol, 165, 104, https://doi.org/10/gj35br, 2018.

Lombard, F., Labeyrie, L., Michel, E., Bopp, L., Cortijo, E., Retailleau, S., Howa, H., and Jorissen, F.: Modelling planktic foraminifer growth and distribution using an ecophysiological multi-species approach, Biogeosciences, 8, 853–873, https://doi.org/10.5194/bg-8-853-2011, 2011.

Marsh, R., Müller, S. A., Yool, A., and Edwards, N. R.: Incorporation of the C-GOLDSTEIN efficient climate model into the GENIE framework: "eb_go_gs" configurations of GENIE, Geoscientific Model Development, 4, 957–992, https://doi.org/10.5194/gmd-4-957-2011, 2011.

Meyer, K. M., Kump, L. R., and Ridgwell, A.: Biogeochemical controls on photic-zone euxinia during the end-Permian mass extinction, Geol, 36, 747, https://doi.org/10.1130/G24618A.1, 2008.

Mitra, A., Flynn, K. J., Tillmann, U., Raven, J. A., Caron, D., Stoecker, D. K., Not, F., Hansen, P. J., Hallegraeff, G., Sanders, R., Wilken, S., McManus, G., Johnson, M., Pitta, P., Våge, S., Berge, T., Calbet, A., Thingstad, F., Jeong, H. J., Burkholder, J., Glibert, P. M., Granéli, E., and Lundgren, V.: Defining Planktonic Protist Functional Groups on Mechanisms for Energy and Nutrient Acquisition: Incorporation of Diverse Mixotrophic Strategies, Protist, 167, 106–120, https://doi.org/10/f3p5h2, 2016.

Monteiro, F. M., Follows, M. J., and Dutkiewicz, S.: Distribution of diverse nitrogen fixers in the global ocean, Global Biogeochem. Cycles, 24, n/a-n/a, https://doi.org/10/ctkc4h, 2010.

Moore, J. K., Doney, S. C., Kleypas, J. A., Glover, D. M., and Fung, I. Y.: An intermediate complexity marine ecosystem model for the global domain, Deep Sea Research Part II: Topical Studies in Oceanography, 49, 403–462, https://doi.org/10/bp99zn, 2001.

Ohman, M. D.: A sea of tentacles: optically discernible traits resolved from planktonic organisms in situ, ICES Journal of Marine Science, 76, 1959–1972, https://doi.org/10.1093/icesjms/fsz184, 2019.

Ortiz, J. D., Mix, A. C., and Collier, R. W.: Environmental control of living symbiotic and asymbiotic foraminifera of the California Current, Paleoceanography, 10, 987–1009, https://doi.org/10/ft8jc7, 1995.

Pianosi, F. and Wagener, T.: A simple and efficient method for global sensitivity analysis based on cumulative distribution functions, Environmental Modelling & Software, 67, 1–11, https://doi.org/10/f677qs, 2015.

Quéré, C. L., Harrison, S. P., Prentice, I. C., Buitenhuis, E. T., Aumont, O., Bopp, L., Claustre, H., Cunha, L. C. D., Geider, R., Giraud, X., Klaas, C., Kohfeld, K. E., Legendre, L., Manizza, M., Platt, T., Rivkin, R. B., Sathyendranath, S., Uitz, J., Watson, A. J., and Wolf-Gladrow, D.: Ecosystem dynamics based on plankton functional types for global ocean biogeochemistry models, Global Change Biology, 11, 2016–2040, https://doi.org/10/cm9nzc, 2005.

R Core Team: R: A Language and Environment for Statistical Computing, R Foundation for Statistical Computing, Vienna, Austria, 2021.

785 Rae, J. W. B., Gray, W. R., Wills, R. C. J., Eisenman, I., Fitzhugh, B., Fotheringham, M., Littley, E. F. M., Rafter, P. A., Rees-Owen, R., Ridgwell, A., Taylor, B., and Burke, A.: Overturning circulation, nutrient limitation, and warming in the Glacial North Pacific, Science Advances, 6, eabd1654, https://doi.org/10/ghrj7m, 2020.

Renaud, S. and Schmidt, D. N.: Habitat tracking as a response of the planktic foraminifer Globorotalia truncatulinoides to environmental fluctuations during the last 140 kyr, Marine Micropaleontology, 49, 97–122, https://doi.org/10/bgp3cz, 2003.

790 Ridgwell, A. and Hargreaves, J. C.: Regulation of atmospheric CO_2 by deep-sea sediments in an Earth system model: REGULATION OF CO_2 BY DEEP-SEA SEDIMENTS, Global Biogeochem. Cycles, 21, n/a-n/a, https://doi.org/10.1029/2006GB002764, 2007.

Ridgwell, A. and Schmidt, D. N.: Past constraints on the vulnerability of marine calcifiers to massive carbon dioxide release, Nature Geosci, 3, 196–200, https://doi.org/10.1038/ngeo755, 2010.

795 Ridgwell, A., Hargreaves, J. C., Edwards, N. R., Annan, J. D., Lenton, T. M., Marsh, R., Yool, A., and Watson, A.: Marine geochemical data assimilation in an efficient Earth System Model of global biogeochemical cycling, Biogeosciences, 4, 87–104, https://doi.org/10/dcq62d, 2007.

Roy, T., Lombard, F., Bopp, L., and Gehlen, M.: Projected impacts of climate change and ocean acidification on the global biogeography of planktonic Foraminifera, Biogeosciences, 12, 2873–2889, https://doi.org/10/f7gcgw, 2015.

800 Salter, I., Schiebel, R., Ziveri, P., Movellan, A., Lampitt, R., and Wolff, G. A.: Carbonate counter pump stimulated by natural iron fertilization in the Polar Frontal Zone, Nature Geoscience, 7, 885–889, https://doi.org/10.1038/ngeo2285, 2014.

Sarrazin, F., Pianosi, F., and Wagener, T.: Global Sensitivity Analysis of environmental models: Convergence and validation, Environmental Modelling & Software, 79, 135–152, https://doi.org/10/f8n8kp, 2016.

Schiebel, R.: Planktic foraminiferal sedimentation and the marine calcite budget, Global Biogeochemical Cycles, 16, 3-1-3–805 21, https://doi.org/10/bdxfhs, 2002.

Schiebel, R. and Hemleben, C.: Planktic Foraminifers in the Modern Ocean, Springer Berlin Heidelberg, Berlin, Heidelberg, https://doi.org/10.1007/978-3-662-50297-6, 2017.

Schiebel, R. and Movellan, A.: First-order estimate of the planktic foraminifer biomass in the modern ocean, Earth System Science Data, 4, 75–89, https://doi.org/10.5194/essd-4-75-2012, 2012.

810 Schmidt, D. N., Thierstein, H. R., Bollmann, J., and Schiebel, R.: Abiotic Forcing of Plankton Evolution in the Cenozoic, Science, 303, 207–210, https://doi.org/10/b37mvn, 2004a.

Schmidt, D. N., Renaud, S., Bollmann, J., Schiebel, R., and Thierstein, H. R.: Size distribution of Holocene planktic foraminifer assemblages: biogeography, ecology and adaptation, Marine Micropaleontology, 50, 319–338, https://doi.org/10/b6nqrj, 2004b.

815 van Sebille, E., Scussolini, P., Durgadoo, J. V., Peeters, F. J. C., Biastoch, A., Weijer, W., Turney, C., Paris, C. B., and Zahn, R.: Ocean currents generate large footprints in marine palaeoclimate proxies, Nat Commun, 6, 6521, https://doi.org/10/f67xqv, 2015.

Séférian, R., Berthet, S., Yool, A., Palmiéri, J., Bopp, L., Tagliabue, A., Kwiatkowski, L., Aumont, O., Christian, J., Dunne, J., Gehlen, M., Ilyina, T., John, J. G., Li, H., Long, M. C., Luo, J. Y., Nakano, H., Romanou, A., Schwinger, J., Stock, C., 820 Santana-Falcón, Y., Takano, Y., Tjiputra, J., Tsujino, H., Watanabe, M., Wu, T., Wu, F., and Yamamoto, A.: Tracking

Improvement in Simulated Marine Biogeochemistry Between CMIP5 and CMIP6, Curr Clim Change Rep, 6, 95–119, https://doi.org/10.1007/s40641-020-00160-0, 2020.

Siccha, M. and Kucera, M.: ForCenS, a curated database of planktonic foraminifera census counts in marine surface sediment samples, Sci Data, 4, 170109, https://doi.org/10.1038/sdata.2017.109, 2017.

825   Silge, J., Chow, F., Kuhn, M., and Wickham, H.: rsample: General resampling infrastructure, 2021.

Spero, H. J. and Parker, S. L.: Photosynthesis in the symbiotic planktonic foraminifer Orbulina universa, and its potential contribution to oceanic primary productivity, Journal of Foraminiferal Research, 15, 273–281, https://doi.org/10/c2rt2q, 1985.

Suggett, D. J., Warner, M. E., and Leggat, W.: Symbiotic Dinoflagellate Functional Diversity Mediates Coral Survival under
830   Ecological Crisis, Trends in Ecology & Evolution, 32, 735–745, https://doi.org/10.1016/j.tree.2017.07.013, 2017.

Sunagawa, S., Acinas, S. G., Bork, P., Bowler, C., Eveillard, D., Gorsky, G., Guidi, L., Iudicone, D., Karsenti, E., Lombard, F., Ogata, H., Pesant, S., Sullivan, M. B., Wincker, P., and de Vargas, C.: Tara Oceans: towards global ocean ecosystems biology, Nat Rev Microbiol, 18, 428–445, https://doi.org/10.1038/s41579-020-0364-5, 2020.

Takagi, H., Kimoto, K., Fujiki, T., Saito, H., Schmidt, C., Kucera, M., and Moriya, K.: Characterizing photosymbiosis in
835   modern planktonic foraminifera, Biogeosciences, 16, 3377–3396, https://doi.org/10/gj35bq, 2019.

Takahashi, K. and Be, A. W. H.: Planktonic foraminifera: factors controlling sinking speeds, Deep Sea Research Part A. Oceanographic Research Papers, 31, 1477–1500, https://doi.org/10.1016/0198-0149(84)90083-9, 1984.

Tierney, J. E., Poulsen, C. J., Montañez, I. P., Bhattacharya, T., Feng, R., Ford, H. L., Hönisch, B., Inglis, G. N., Petersen, S. V., Sagoo, N., Tabor, C. R., Thirumalai, K., Zhu, J., Burls, N. J., Foster, G. L., Goddéris, Y., Huber, B. T., Ivany, L. C.,
840   Kirtland Turner, S., Lunt, D. J., McElwain, J. C., Mills, B. J. W., Otto-Bliesner, B. L., Ridgwell, A., and Zhang, Y. G.: Past climates inform our future, Science, 370, eaay3701, https://doi.org/10/gh6c3g, 2020.

Todd, C. L., Schmidt, D. N., Robinson, M. M., and Schepper, S. D.: Planktic Foraminiferal Test Size and Weight Response to the Late Pliocene Environment, Paleoceanography and Paleoclimatology, 35, e2019PA003738, https://doi.org/10/ghrd4r, 2020.

845   Tréguer, P., Bowler, C., Moriceau, B., Dutkiewicz, S., Gehlen, M., Aumont, O., Bittner, L., Dugdale, R., Finkel, Z., Iudicone, D., Jahn, O., Guidi, L., Lasbleiz, M., Leblanc, K., Levy, M., and Pondaven, P.: Influence of diatom diversity on the ocean biological carbon pump, Nature Geoscience, 11, 27–37, https://doi.org/10/gcxznd, 2018.

Uhle, M. E., Macko, S. A., Spero, H. J., Lea, D. W., Ruddiman, W. F., and Engel, M. H.: The fate of nitrogen in the Orbulina universa foraminifera-symbiont system determined by nitrogen isotope analyses of shell-bound organic matter,
850   Limnol. Oceanogr., 44, 1968–1977, https://doi.org/10/ffgtfw, 1999.

Våge, S., Castellani, M., Giske, J., and Thingstad, T. F.: Successful strategies in size structured mixotrophic food webs, Aquat Ecol, 47, 329–347, https://doi.org/10.1007/s10452-013-9447-y, 2013.

van de Velde, S. J., Hülse, D., Reinhard, C. T., and Ridgwell, A.: Iron and sulfur cycling in the cGENIE.muffin Earth system model (v0.9.21), Geosci. Model Dev., 14, 2713–2745, https://doi.org/10.5194/gmd-14-2713-2021, 2021.

855   Ward, B. A. and Follows, M. J.: Marine mixotrophy increases trophic transfer efficiency, mean organism size, and vertical carbon flux, Proc Natl Acad Sci USA, 113, 2958–2963, https://doi.org/10/ggnmm5, 2016.

Ward, B. A., Wilson, J. D., Death, R. M., Monteiro, F. M., Yool, A., and Ridgwell, A.: EcoGEnIE 1.0: plankton ecology in the cGEnIE Earth system model, Geosci. Model Dev., 11, 4241–4267, https://doi.org/10/gfjrbk, 2018.

Watanabe, S., Hajima, T., Sudo, K., Nagashima, T., Takemura, T., Okajima, H., Nozawa, T., Kawase, H., Abe, M., Yokohata, T., Ise, T., Sato, H., Kato, E., Takata, K., Emori, S., and Kawamiya, M.: MIROC-ESM 2010: model description and basic results of CMIP5-20c3m experiments, Geoscientific Model Development, 4, 845–872, https://doi.org/10.5194/gmd-4-845-2011, 2011.

Waterson, A. M., Edgar, K. M., Schmidt, D. N., and Valdes, P. J.: Quantifying the stability of planktic foraminiferal physical niches between the Holocene and Last Glacial Maximum: Niche Stability of Planktic Foraminifera, Paleoceanography, 32, 74–89, https://doi.org/10/f9vbtb, 2017.

Watterson, I. G.: Non-Dimensional Measures of Climate Model Performance, International Journal of Climatology, 16, 379–391, https://doi.org/10.1002/(SICI)1097-0088(199604)16:4<379::AID-JOC18>3.0.CO;2-U, 1996.

Watterson, I. G., Bathols, J., and Heady, C.: What Influences the Skill of Climate Models over the Continents?, Bulletin of the American Meteorological Society, 95, 689–700, https://doi.org/10.1175/BAMS-D-12-00136.1, 2014.

West, G. B., Brown, J. H., and Enquist, B. J.: A General Model for the Origin of Allometric Scaling Laws in Biology, Science, 276, 122–126, https://doi.org/10.1126/science.276.5309.122, 1997.

Wilson, J. D., Andrews, O., Katavouta, A., de Melo Viríssimo, F., Death, R. M., Adloff, M., Baker, C. A., Blackledge, B., Goldsworth, F. W., Kennedy-Asser, A. T., Liu, Q., Sieradzan, K. R., Vosper, E., and Ying, R.: The biological carbon pump in CMIP6 models: 21st century trends and uncertainties, Proc. Natl. Acad. Sci. U.S.A., 119, e2204369119, https://doi.org/10.1073/pnas.2204369119, 2022.

Zakharova, L., Meyer, K. M., and Seifan, M.: Trait-based modelling in ecology: A review of two decades of research, Ecological Modelling, 407, 108703, https://doi.org/10.1016/j.ecolmodel.2019.05.008, 2019.

Žarić, S., Schulz, M., and Mulitza, S.: Global prediction of planktic foraminiferal fluxes from hydrographic and productivity data, Biogeosciences, 3, 187–207, https://doi.org/10/ddgc7j, 2006.